Polar Geosci , 13, 60-85, 2000

Ultrahigh-temperature metamorphic rocks from Howard Hills in the Napier Complex, East Antarctica

Yasutaka Yoshimura[1], Yoichi Motoyoshi[2], Edward S Grew[3], Tomoharu Miyamoto[4], Christopher J Carson[5] and Daniel J Dunkley[6]*

[1]*Department of Natural Environmental Science, Kochi University, Akebono-cho 2-5-1, Kochi 780-8520*
[2]*National Institute of Polar Research, Kaga 1-9-10, Itabashi-ku, Tokyo 173-8515*
[3]*Department of Geological Science, University of Maine, 5790 Bryand Research Center, Orono, Maine, 04469-5790, U S A*
[4]*Department of Earth and Planetary Science, Kyushu University, Hakozaki 6-10-1, Fukuoka 812-8581*
[5]*Department of Geology and Geophysics, Kline Geology Laboratory, Yale University, 210 Whitney Ave , New Haven, CT 06511, U S A*
[6]*Gamagori Natural History of Museum, Minato-cho 17-17, Gamagori 443-0034*

Abstract: The Howard Hills area consists predominantly of garnet felsic gneiss, orthopyroxene felsic gneiss and aluminous gneiss which contain garnet, sapphirine and sillimanite in various amounts The characteristic assemblage of sapphirine+quartz is present in quartzo-feldspathic layers within the aluminous gneiss The peak metamorphic conditions are estimated to have been about 1150-1200°C The condition is obtained by plotting the inferred original compositions of mesoperthites from the garnet felsic gneiss, orthopyroxene felsic gneiss, and aluminous gneiss on an An-Ab-Or ternary diagram, the original composition of the mesoperthites is derived by multiplying the modal ratio of host and lamella by their respective chemical compositions Probable P-T conditions for retrograde metamorphism are estimated using garnet-orthopyroxene isopleths, and range from 830 to 950°C and 5 to 9 5 kbar Quartz inclusions in the cores of garnets from silica-undersaturated layers within the aluminous gneiss indicate the medium in which the garnets crystallized under the silica-oversaturated condition This implies mass transfer within the aluminous gneiss, probably involving partial melting that also led to high Y concentrations in garnet cores, high An values for plagioclase, and high Ba contents in mesoperthites from the aluminous gneiss Partial melt from aluminous gneiss was generated during prograde metamorphism and segregated, the restite might have undergone continuous ultrahigh-temperature metamorphism

key words UHT metamorphic rocks, UHT metamorphism, Howard Hills, Napier Complex, partial melting

*Present address Division of Geology and Geophysics, School of Geosciences, University of Sydney, NSW 2006, Australia

1. Introduction

The Napier complex is an ultrahigh-temperature (UHT) metamorphic terrane characterized by mineral assemblages such as sapphirine+quartz, orthopyroxene+sillimanite+quartz, and osumilite (*e.g*, Sheraton *et al*, 1987, Harley and Hensen, 1990). Timing of metamorphism has been dated at ca. 2.4–2 5 Ga (*e.g*., Grew and Manton, 1979, Owada *et al*, 1994, Tainosho *et al*, 1994, Shiraishi *et al*, 1997, Asami *et al*, 1998) and SHRIMP age results for the rocks are ca 3 93 Ga (Black *et al*, 1986) to 3.95 Ga (Williams *et al*, 1984) This complex can therefore provide important information for our understanding of the development and evolution of continental crust in the Archaean to early Paleoproterozoic

Investigation of the Napier Complex was carried out by the JARE (Japanese Antarctic Research Expedition) under the SEAL (Structure and Evolution of east Antarctic Lithosphere) project, started in 1996 The first and second seasons focused on detailed geological surveying of the study area by JARE-38 (1996–1997) in the Mt Riiser-Larsen area (Ishizuka *et al*, 1998) and JARE-39 (1997–1998) in the Tonagh Island area (Osanai *et al*, 1999), respectively. In both areas, petrological, geochemical, geochronological and structural investigations were carried out (*e.g*, Toyoshima *et al*., 1999, Hokada *et al*, 1999a; Tsunogae *et al*., 1999, Owada *et al*, 1999, Suzuki *et al*, 1999) In JARE-40 (1998–1999), an extensive geological investigation using a helicopter was undertaken in the Amundsen Bay region including the Howard Hills, an area that had not previously been explored by JARE This paper describes the ultrahigh-temperature metamorphic rocks from the Howard Hills, and interprets their implications for UHT-metamorphism and partial melting.

2. Geological outline and petrography

The Howard Hills area is located about 30 km east of Tonagh Island in the west-central part of the Napier complex, Enderby Land, East Antarctica (Fig 1) The Howard Hills consist of an east-west mountain ridge that is bounded on the north by the Beaver Glacier and on the west, south and east by continental ice sheets. According to the compilation data of Harley and Hensen (1990), the Howard Hills area represents a very high-temperature region characterized by the mineral assemblages sapphirine+quartz and orthopyroxene+sillimanite The geological survey was focused on the northern part of the Howard Hills. The study area is composed of layered gneisses of various origins and bulk chemistries Garnet felsic gneiss and orthopyroxene felsic gneiss are the most abundant rock types in this area An aluminous gneiss that is rich in garnet, sapphirine and sillimanite is present within the garnet felsic gneiss as layers of variable thickness Minor amounts of metamorphosed ultramafic rocks are also present as blocks, lenses and thin layers within the garnet felsic gneiss and orthopyroxene felsic gneiss (Fig 2) Unmetamorphosed doleritic intrusive rocks (Amundsen Dikes) are also present in the area In this paper, the garnet felsic gneisses, aluminous gneisses and orthopyroxene felsic gneisses are described

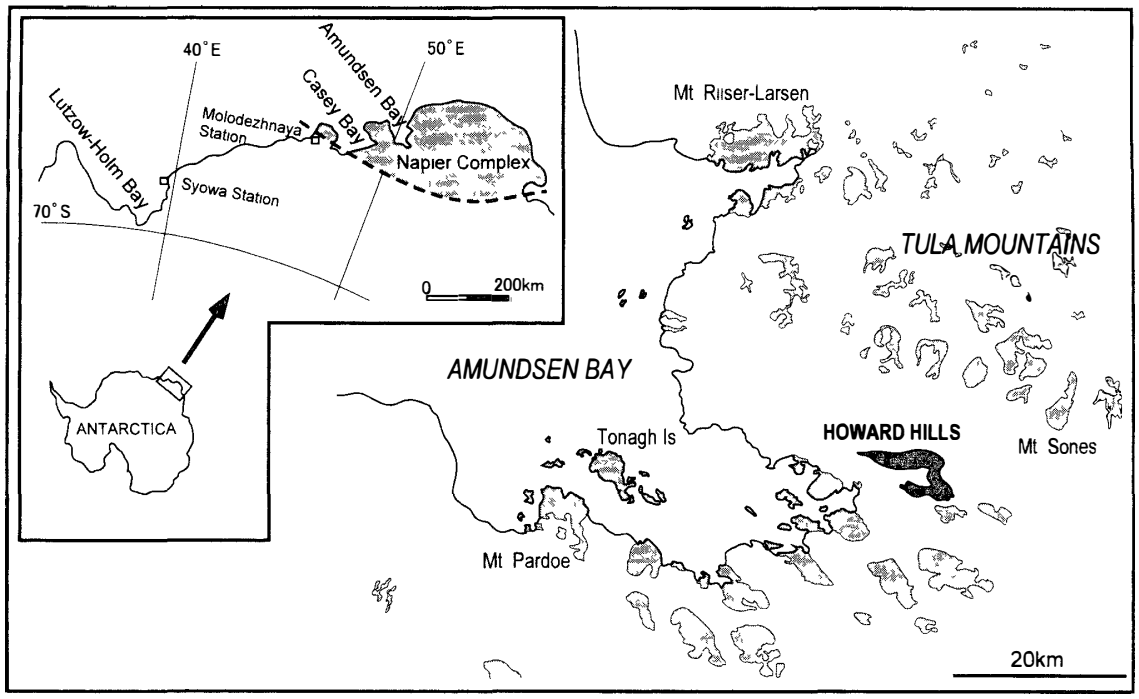

Fig 1 Location map of the Howard Hills in Enderby Land, East Antarctica

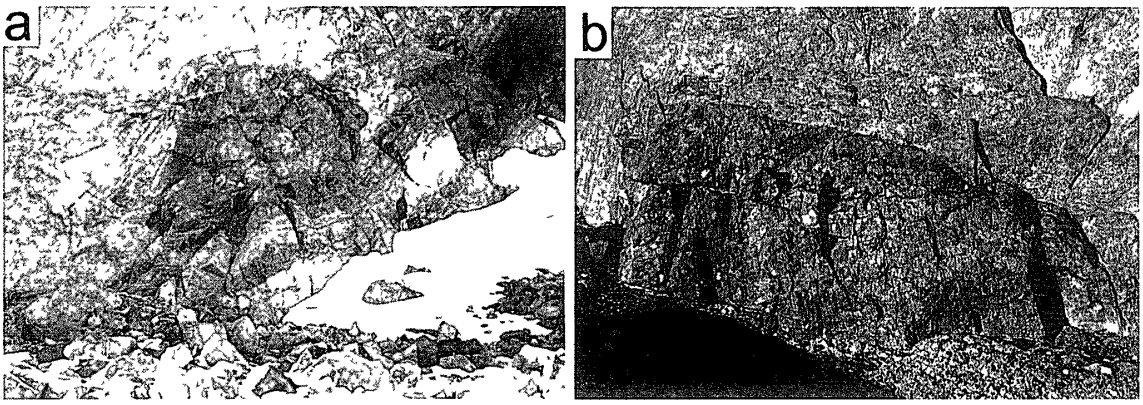

Fig 2 (a) Lenticular metamorphosed ultramafic rock embeded within the garnet felsic gneiss (b) Pyroxenite block within the orthopyroxene felsic gneiss

2 1. Garnet felsic gneiss

Garnet felsic gneiss is widespread in the studied area Figure 3 shows characteristic field exposure, polished slab, and thin section views of the garnet felsic gneiss This gneiss is rich in coarsely crystalline garnet porphyroblast (diameter up to 3 cm), alkali feldspar, plagioclase and quartz, and contains small amounts of spinel and rutile Sapphirine is rare, and comparatively fine-grained, it is light green in plane-polarized light, and commonly contains inclusions of sillimanite, plagioclase, and quartz Spinel is often included Orthopyroxene is absent The main mineral assemblages are as follows

garnet + sillimanite + mesoperthite + plagioclase + quartz
garnet + sillimanite + sapphirine + mesoperthite + plagioclase
garnet + sillimanite + spinel + mesoperthite + plagioclase

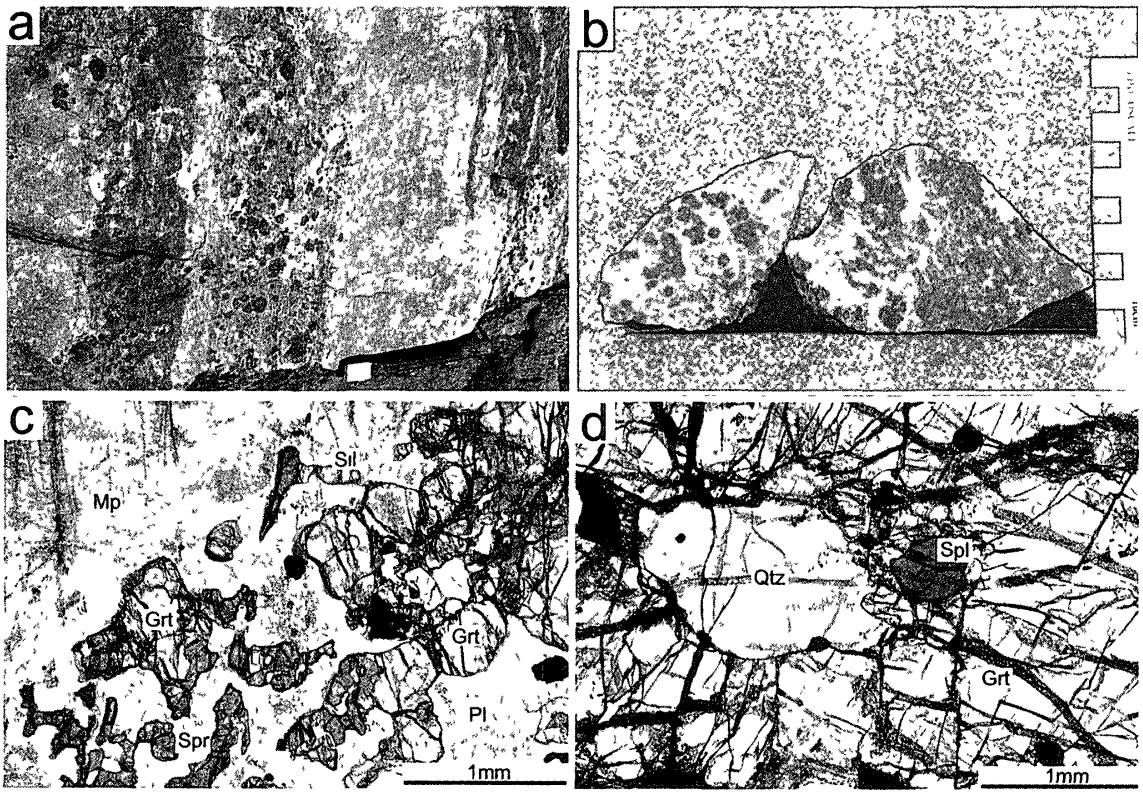

Fig 3 Representative photographs of outcrop (a), polished slab (b) and thin section views (c and d) of Howard Hills rocks Spinel and quartz inclusions in garnet are in close proximity to one another (d) Grt garnet, Spr sapphirine, Sil. sillimanite, Pl. plagioclase, Mp mesoperthite, Spl spinel, Qtz quartz

Though coexisting sapphirine+quartz or spinel+quartz is not recognized in the matrix, spinel and quartz inclusions in garnet are commonly in very close proximity to one another (Fig 3d)

2.2. Aluminous gneiss

As shown in Fig 4, the aluminous gneiss is rich in garnet, sapphirine and sillimanite, and is found in garnet felsic gneiss as layers several cm to 30 cm thick The aluminous gneiss lithofacies are variable in composition and appearance A representative field exposure is shown in Fig 4 The main aluminous gneiss rock types are as follows

Type-A Rich in coarsely crystalline garnet (about 1 5–2 cm diameter), sapphirine, and sillimanite, with spinel, plagioclase, and alkali-feldspar Quartz is absent (Fig 5a)

Type-B Aluminous layers rich in comparatively finely crystalline garnet (about 1–7 mm), sapphirine and sillimanite, with cordierite, plagioclase, and alkali-feldspar Quartz is absent These aluminous layers are intercalated with felsic layers that contain finely crystalline garnet (1 mm or smaller) and sapphirine (Fig. 6a)

Type-C Finely crystalline garnet (about 0 3–0 5 mm), sapphirine, spinel, plagioclase, and alkali-feldspar$\pm$quartz (relatively felsic compared to types-A and -B) is interlayered with quartzo-feldsparthic layers (Fig 7a)

Typical polished slabs and photomicrographs of each rock type are shown in Figs 5–

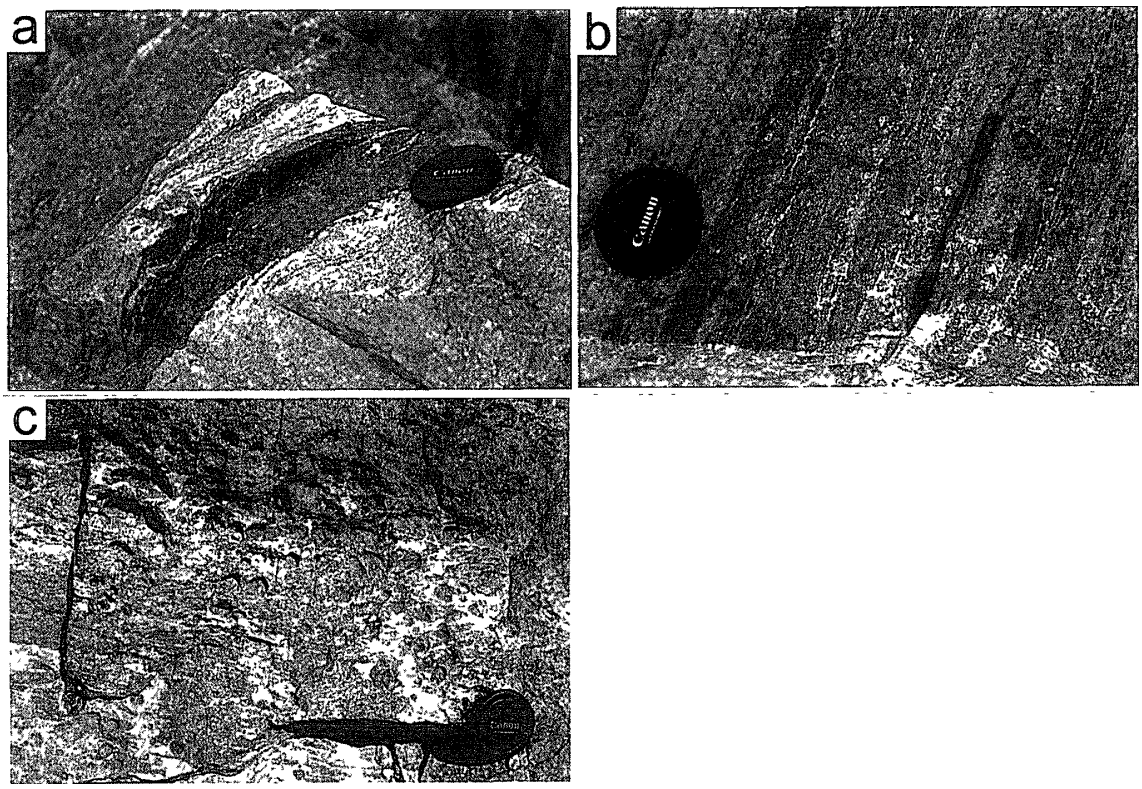

Fig 4 Representative field photographs of aluminous gneisses from Howard Hills (a) Aluminous gneiss interlayered with garnet felsic gneiss (type-A) (b) Aluminous gneiss interlayered with garnet felsic gneiss (type-B) (c) Rich in garnet, sapphirine, spinel and sillimanite and relatively felsic and weakly gneissose relative to other types of aluminous gneiss (type-C)

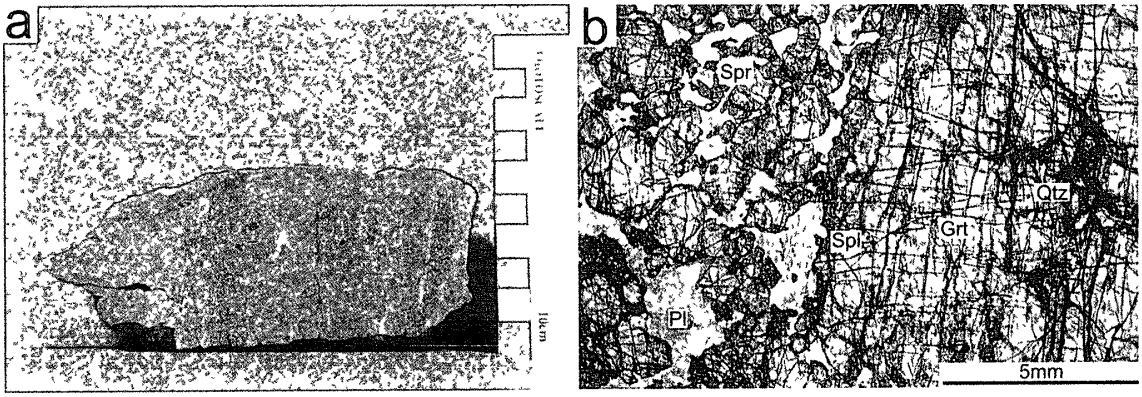

Fig 5 Type-A aluminous gneiss (a) Polished surface (b) Photomicrograph of thin section Garnet has quartz inclusions, and sapphirine has spinel inclusions

7 Orthopyroxene is rare in all of these rock types, it is present in type-B as inclusions in garnet and cordierite, at the margins of garnet crystals, and in intergranular areas between cordierite masses (Fig 6d) Orthopyroxene and cordierite are secondarily minerals, and orthopyroxene and sillimanite are not stable assemblages at ultrahigh-temperature (Fig 6d) Spinel is often included in sapphirine within type-A aluminous gneiss Although

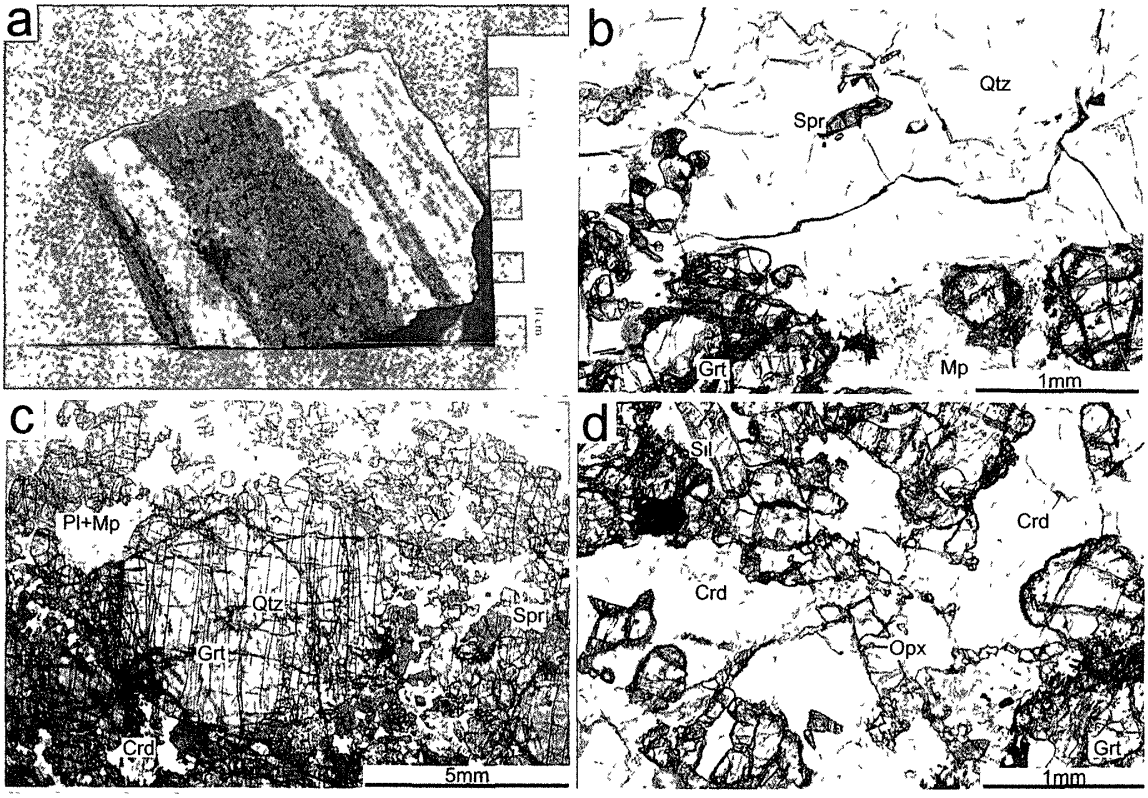

Fig 6 Polished surface and thin section photomicrograph of type-B aluminous gneiss from Howard Hills (a) Polished surface (b) Sapphirine and quartz in a quartzo-feldspathic layer (c) Quartz inclusions in garnet It is noteworthy that quartz is free in the matrix (d) Orthopyroxene along a cordierite grain boundary Opx orthopyroxene, Crd cordierite

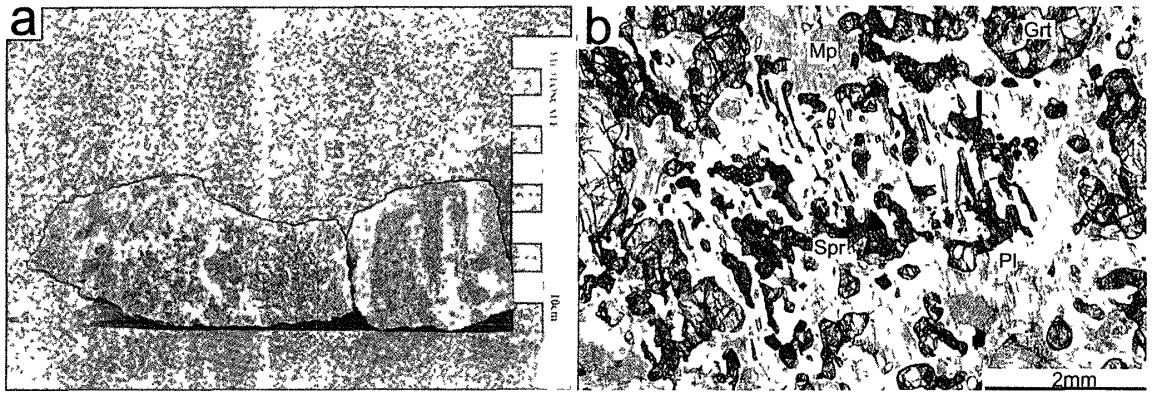

Fig 7 Polished surface and photomicrograph of type-C aluminous gneiss from Howard Hills (a) Polished surface (b) Acicular sapphirines

quartz is absent in the matrix of aluminous layer of type-A and type-B aluminous gneiss, quartz inclusions are present in the core of garnets (Fig 5b, 6c) The assemblage sapphirine+quartz is present in the quartzo-feldspathic layers of rock type-B (Fig 6b) Coarsely crystalline sapphirine commonly occurs as prisms in type-B aluminous gneiss, and as acicular crystals in type-C aluminous gneiss (Fig 7b) Sapphirine is light green in plane-polarized light in all rock types The main mineral assemblages of each type are as follows

Type-A

garnet + sillimanite + plagioclase + perthite + sapphirine + spinel
garnet + sillimanite + plagioclase + perthite + sapphirine
garnet + sillimanite + plagioclase + perthite + spinel
garnet + sillimanite + plagioclase + sapphirine + spinel

Type-B, felsic layer

garnet + plagioclase + mesoperthite + quartz
garnet + sapphirine + plagioclase + mesoperthite + quartz
garnet + sillimanite + plagioclase + mesoperthite + quartz
garnet + sapphirine + orthopyroxene + plagioclase + mesoperthite + quartz
garnet + sillimanite + sapphirine + plagioclase + mesoperthite + quartz

Type-B, alumınous layer

garnet + sillimanite + sapphirine + cordierite + plagioclase + mesoperthite
garnet + sapphirine + orthopyroxene + cordierite + plagioclase + mesoperthite
garnet + sillimanite + sapphirine + cordierite + plagioclase

Type-C

garnet + sillimanite + sapphirine + spinel + plagioclase + mesoperthite
garnet + sillimanite + sapphirine + plagioclase + mesoperthite
garnet + sillimanite + spinel + mesoperthite + plagioclase
garnet + sillimanite + plagioclase + mesoperthite + quartz

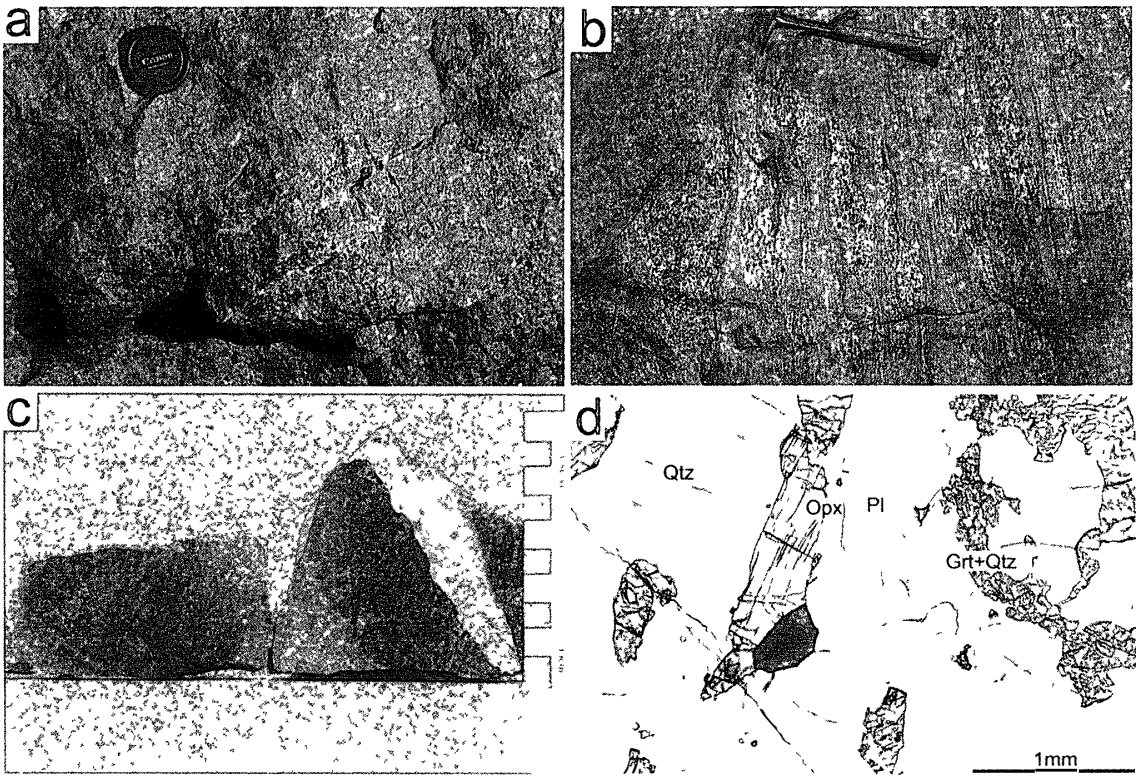

Fig 8 Orthopyroxene felsic gneiss from Howard Hills (a) and (b) Overview of the outcrop Well-developed compositional layering observed in orthopyroxene felsic gneiss (c) Polished surface (d) Photomicrograph of thin section Note symplectitic intergrowth of quartz and garnet

2.3. Orthopyroxene felsic gneiss

Orthopyroxene felsic gneiss is also widespread in the area and preserves compositional layering This gneiss is composed of orthopyroxene, plagioclase, alkali-feldspar and quartz (dark), with rare garnet. Representative field exposure, polished slab and thin-section views are shown in Fig 8 Most garnets show some intergrowth with quartz (Fig 8d) Orthopyroxene is absent from any domain (about 1 to 3 cm in size) containing relatively coarse-grained garnet. The main mineral assemblages are as follows

orthopyroxene+garnet+plagioclase+perthite to mesoperthite+quartz
orthopyroxene+plagioclase+perthite to mesoperthite+quartz
garnet+plagioclase+perthite+quartz (limited to domains containing coarse grained garnet)

3. Mineral chemistry

3.1. Analytical techniques

Mineral chemical compositions were obtained using a wave-length dispersive electron probe microanalyzer (JEOL JXA-8600M) at Kochi University For quantitative analyses, an acceleration voltage of 15 kV, probe current of 1.5×10^{-8} A, and beam diameter of 1 or 5 μm were used. Oxide ZAF correction was applied to the data For compositional mapping, an acceleration voltage of 15 kV (major elements) or 25 kV (Y and Yb), probe current of 7.5×10^{-7} A (major elements) or 8×10^{-7} A (Y and Yb), dwell time of 50 ms (major elements) or 250 ms (Y and Yb) and beam diameter of 5 μm were used The compositions of the analyzed minerals are shown in Table 1.

3.2. Mineral compositions

3 2 1. Garnet

Prp-Alm-Sps and Prp-Alm-Grs diagrams for garnet are shown in Fig. 9, and typical color maps are shown in Fig 10 In the garnet felsic gneiss, garnets that coexist with sapphirine have $Alm_{44-49}Prp_{51-54}Grs_{2-3}Sps_1$ as the core compositions, whereas garnets in the sapphirine-free domain have $Alm_{54-58}Prp_{41-44}Grs_{2-3}Sps_1$ in the core compositions Garnet core compositions from type-A and type-C aluminous gneisses are $Alm_{42-45}Prp_{51-55}Grs_{4-5}Sps_1$ and $Alm_{45-47}Prp_{50-52}Grs_{2-3}Sps_1$ respectively, and garnets from both aluminous and felsic layers of the type-B aluminous gneiss have $Alm_{41-46}Prp_{52-57}Grs_{3-4}Sps_1$ In the orthopyroxene felsic gneiss, the core composition of garnets coexisting with orthopyroxene is $Alm_{62-65}Prp_{28-31}Grs_{6-7}Sps_{1-2}$, whereas garnets in the orthopyroxene-free domain have $Alm_{67-69}Prp_{24-27}Grs_{6-7}Sps_{1-2}$, which are low values compared to those of the other rock types The spessartine content of all rock types ranges from 0 5 to 0.8 In all of the rock types, composition does not vary with crystal size Mg contents are highest in cores and gradually decrease towards rims Zoning of the major element composition formed during cooling and reflects high-temperature diffusion Grossular content varies with rock type, such that garnets of types-A and -B aluminous gneisses show higher Grs values than those of the garnet felsic gneiss or type-C aluminous gneiss Grossular values of garnets from the orthopyroxene felsic gneiss are higher than those of garnets from the other rock types The Y and Yb contents of garnets with quartz inclusions in types-A and -B aluminous gneisses are highest in cores and decrease toward rims (Fig 10) The Y content

Table 1 Representative electron microprobe analyses of minerals in garnet felsic gneiss, aluminous gneiss and orthopyroxene felsic gneiss from Howard Hills Fe^{3+} of sapphirine was obtained by stoichiometric calculation (O = 20) using the method of Higgins et al (1979)

mineral	Garnet (O=12)																				
rock type	Grt-felsic gn						Type-A			Type-B						Type-C			Opx-felsic gn		
sample	9812290202			9812290403			9812280101			9812290501				9812290507S		9812290101			9812290801S		
SiO_2	39 92	39 94	39 76	39 46	39 11	39 09	40 43	40 36	40 09	40 98	41 07	41 03	40 14	40 95	41 04	40 25	39 92	40 03	38 85	38 77
TiO_2	0 04	0 02	0 00	0 01	0 03	0 03	0 02	0 00	0 00	0 06	0 00	0 00	0 02	0 02	0 00	0 00	0 01	0 01	0 00	0 03
Al_2O_3	22 66	22 78	22 67	22 49	22 17	22 24	23 10	22 85	22 91	22 96	23 16	23 03	22 93	22 90	23 02	22 91	22 63	22 71	21 92	21 74
Y_2O_3	0 00	0 05	0 01	0 10	0 05	0 01	0 08	0 16	0 04	0 04	0 04	0 08	0 04	0 04	0 01	0 03	0 00	0 01	0 00	0 00
Yb_2O_3	0 00	0 06	0 00	0 00	0 03	0 03	0 11	0 07	0 00	0 03	0 00	0 11	0 00	0 00	0 05	0 00	0 09	0 00	0 00	0 00
Cr_2O_3	0 09	0 06	0 12	0 15	0 19	0 17	0 29	0 26	0 10	0 16	0 16	0 12	0 33	0 18	0 11	0 19	0 18	0 18	0 00	0 00
FeO*	21 46	22 31	21 99	25 83	25 97	25 91	20 39	21 45	20 89	20 61	20 19	21 11	20 90	20 62	21 21	22 51	22 11	22 37	29 27	28 54
MnO	0 31	0 30	0 26	0 53	0 45	0 53	0 37	0 36	0 40	0 24	0 27	0 32	0 33	0 22	0 26	0 40	0 35	0 31	0 61	0 54
NiO	0 00	0 00	0 00	0 00	0 00	0 00	0 00	0 00	0 00	0 00	0 00	0 00	0 00	0 00	0 00	0 00	0 00	0 00	0 00	0 00
MgO	13 99	13 90	13 89	11 14	10 80	10 99	14 15	14 21	14 11	15 01	15 11	14 69	14 24	14 81	14 98	13 94	13 84	13 47	7 46	7 61
CaO	0 95	0 90	0 93	1 04	0 97	1 05	1 65	1 61	1 57	1 05	1 06	1 21	1 15	1 04	1 09	0 93	1 00	1 00	2 48	2 56
Na_2O	0 00	0 01	0 00	0 00	0 00	0 01	0 00	0 01	0 00	0 02	0 00	0 00	0 02	0 01	0 01	0 01	0 01	0 01	0 00	0 00
K_2O	0 00	0 00	0 00	0 00	0 00	0 00	0 00	0 00	0 00	0 00	0 00	0 00	0 00	0 00	0 00	0 00	0 00	0 00	0 00	0 00
P_2O_5	0 00	0 08	0 08	0 03	0 02	0 05	0 00	0 02	0 01	0 05	0 00	0 03	0 03	0 00	0 03	0 03	0 03	0 02	0 06	0 00
BaO	n d	n d	n d	n d	n d	n d	n d	n d	n d	n d	n d	n d	n d	n d	n d	n d	n d	n d	n d	n d
ZnO	n d	n d	n d	n d	n d	n d	n d	n d	n d	n d	n d	n d	n d	n d	n d	n d	n d	n d	n d	n d
Total	99 42	100 41	99 70	100 78	99 79	100 10	100 58	101 37	100 11	101 22	101 05	101 72	100 13	100 78	101 81	101 22	100 17	100 13	100 64	99 80
Si	2 991	2 975	2 978	2 982	2 989	2 978	2 987	2 975	2 981	2 999	3 004	2 998	2 981	3 010	2 995	2 976	2 981	2 990	3 001	3 012
Ti	0 002	0 001	0 000	0 001	0 002	0 001	0 001	0 000	0 000	0 003	0 000	0 000	0 001	0 001	0 000	0 000	0 000	0 001	0 000	0 002
Al	2 001	2 000	2 001	2 003	1 997	1 997	2 012	1 986	2 008	1 981	1 997	1 984	2 007	1 983	1 979	1 997	1 992	2 000	1 995	1 991
Fe^{3+}	-	-	-	-	-	-	-	-	-	-	-	-	-	-	-	-	-	-	-	-
Y	0 000	0 002	0 000	0 004	0 002	0 000	0 003	0 006	0 001	0 002	0 001	0 003	0 002	0 002	0 000	0 001	0 000	0 000	0 000	0 000
Yb	0 000	0 001	0 000	0 000	0 001	0 001	0 002	0 002	0 000	0 001	0 000	0 002	0 000	0 000	0 001	0 000	0 002	0 000	0 000	0 000
Cr	0 006	0 004	0 007	0 009	0 012	0 010	0 017	0 015	0 006	0 009	0 009	0 007	0 020	0 010	0 007	0 011	0 011	0 011	0 000	0 000
Fe^{2+}	1 345	1 390	1 377	1 632	1 660	1 651	1 260	1 322	1 299	1 261	1 235	1 290	1 298	1 267	1 294	1 392	1 381	1 398	1 891	1 855
Mn	0 020	0 019	0 016	0 034	0 029	0 034	0 023	0 023	0 025	0 015	0 017	0 020	0 021	0 014	0 016	0 025	0 022	0 020	0 040	0 036
Ni	0 000	0 000	0 000	0 000	0 000	0 000	0 000	0 000	0 000	0 000	0 000	0 000	0 000	0 000	0 000	0 000	0 000	0 000	0 000	0 000
Mg	1 562	1 543	1 551	1 255	1 230	1 248	1 558	1 561	1 564	1 638	1 647	1 600	1 576	1 622	1 629	1 537	1 541	1 500	0 859	0 882
Ca	0 076	0 072	0 075	0 084	0 080	0 085	0 131	0 127	0 125	0 083	0 083	0 095	0 092	0 082	0 086	0 074	0 080	0 080	0 205	0 213
Na	0 000	0 002	0 000	0 001	0 000	0 001	0 000	0 002	0 000	0 003	0 000	0 000	0 003	0 001	0 001	0 002	0 002	0 002	0 000	0 000
K	0 000	0 000	0 000	0 000	0 000	0 000	0 000	0 000	0 000	0 000	0 000	0 000	0 000	0 000	0 000	0 000	0 000	0 000	0 000	0 000
P	0 000	0 005	0 005	0 002	0 001	0 003	0 000	0 001	0 001	0 003	0 000	0 002	0 002	0 000	0 002	0 002	0 002	0 001	0 004	0 000
Ba	-	-	-	-	-	-	-	-	-	-	-	-	-	-	-	-	-	-	-	-
Zn	-	-	-	-	-	-	-	-	-	-	-	-	-	-	-	-	-	-	-	-
Total	8 003	8 014	8 011	8 007	8 002	8 011	7 995	8 020	8 010	7 998	7 993	8 002	8 002	7 992	8 010	8 017	8 014	8 002	7 995	7 991
X_{Mg}	0 54	0 53	0 53	0 44	0 43	0 43	0 55	0 54	0 55	0 57	0 57	0 55	0 55	0 56	0 56	0 53	0 53	0 52	0 31	0 32
Prp	52 02	51 03	51 38	41 76	41 03	41 36	52 44	51 47	51 91	54 66	55 24	53 26	52 78	54 35	53 87	50 76	50 96	50 04	28 68	29 54
Alm	44 78	45 96	45 61	54 30	55 35	54 68	42 39	43 59	43 11	42 09	41 41	42 94	43 46	42 45	42 77	45 97	45 67	46 62	63 14	62 12
Sps	0 66	0 62	0 54	1 13	0 97	1 13	0 77	0 74	0 83	0 49	0 57	0 65	0 70	0 45	0 53	0 83	0 72	0 66	1 33	1 20
Grs	2 54	2 39	2 48	2 81	2 65	2 83	4 40	4 20	4 15	2 76	2 78	3 15	3 06	2 75	2 83	2 44	2 65	2 68	6 86	7 14

*=Total Fe as FeO n d not determined

Table 1 Continued

mineral	Garnet (O=12)				Sapphirine (O=20)												
rock type	Opx-felsic gn				Grt-felsic gn			Type-A			Type-B					Type-C		
sample	98122908015		9812291002S		9812290202			9812280101			9812290501			9812290507S		9812290101		
SiO_2	39 12	38 51	38 23	37 95	15 08	14 67	14 87	13 20	13 18	14 24	13 55	13 74	13 24	13 48	13 04	13 02	13 01	13 18
TiO_2	0 01	0 00	0 00	0 00	0 09	0 05	0 05	0 04	0 07	0 06	0 04	0 04	0 06	0 03	0 42	0 03	0 03	0 04
Al_2O_3	22 31	21 67	21 84	21 58	58 21	58 66	58 55	63 36	62 05	61 30	62 76	61 63	61 64	59 69	60 58	63 07	61 90	61 48
Y_2O_3	0 00	0 00	0 00	0 00	n d	n d	n d	n d	n d	n d	n d	n d	n d	n d	n d	n d	n d	n d
Yb_2O_3	0 00	0 00	0 00	0 00	n d	n d	n d	n d	n d	n d	n d	n d	n d	n d	n d	n d	n d	n d
Cr_2O_3	0 00	0 04	0 00	0 00	1 07	1 18	1 12	0 88	1 10	1 02	1 31	1 32	2 00	2 31	2 49	0 79	0 89	0 86
FeO*	28 77	32 22	30 78	31 37	9 04	8 36	8 54	5 73	6 84	7 46	5 58	6 72	5 32	7 36	6 81	7 91	7 39	7 81
MnO	0 49	0 55	0 59	0 54	0 00	0 00	0 00	0 05	0 01	0 01	0 06	0 04	0 06	0 00	0 00	0 03	0 02	0 02
NiO	0 00	0 00	0 00	0 00	0 00	0 00	0 00	0 00	0 00	0 00	0 00	0 00	0 00	0 00	0 00	0 00	0 00	0 00
MgO	8 13	6 14	6 18	6 16	16 24	16 29	16 28	16 88	16 42	16 70	17 10	16 82	17 30	16 41	16 57	15 96	16 24	15 73
CaO	2 41	2 09	2 41	2 45	0 02	0 01	0 01	0 04	0 04	0 00	0 00	0 00	0 01	0 02	0 05	0 00	0 00	0 03
Na_2O	0 01	0 02	0 02	0 01	0 03	0 00	0 00	0 00	0 00	0 00	0 00	0 00	0 00	0 01	0 00	0 01	0 00	0 01
K_2O	0 00	0 00	0 00	0 00	0 00	0 00	0 00	0 00	0 00	0 00	0 00	0 00	0 00	0 00	0 00	0 00	0 00	0 00
P_2O_5	0 00	0 03	0 03	0 04	0 02	0 02	0 00	0 01	0 01	0 00	0 00	0 01	0 00	0 00	0 00	0 00	0 04	0 00
BaO	n d	n d	n d	n d	n d	n d	n d	n d	n d	n d	n d	n d	n d	n d	n d	n d	n d	n d
ZnO	n d	n d	n d	n d	n d	n d	n d	n d	n d	n d	n d	n d	n d	n d	n d	n d	n d	n d
Total	101 26	101 27	100 08	100 08	99 81	99 24	99 43	100 19	99 71	100 79	100 40	100 33	99 62	99 31	99 94	100 83	99 52	99 15
Si	2 992	2 996	2 995	2 984	1 814	1 769	1 791	1 557	1 572	1 682	1 595	1 627	1 574	1 625	1 559	1 541	1 557	1 586
Ti	0 001	0 000	0 000	0 000	0 009	0 004	0 005	0 004	0 006	0 005	0 004	0 004	0 006	0 003	0 038	0 003	0 003	0 004
Al	2 011	1 987	2 016	2 000	8 248	8 338	8 310	8 807	8 721	8 536	8 709	8 606	8 638	8 480	8 541	8 798	8 735	8 722
Fe^{3+}	-	-	-	-	0 023	0 012	0 002	0 000	0 032	0 005	0 000	0 016	0 026	0 051	0 106	0 045	0 066	0 024
Y	0 000	0 000	0 000	0 000	-	-	-	-	-	-	-	-	-	-	-	-	-	-
Yb	0 000	0 000	0 000	0 000	-	-	-	-	-	-	-	-	-	-	-	-	-	-
Cr	0 000	0 002	0 000	0 000	0 102	0 112	0 107	0 082	0 103	0 095	0 122	0 123	0 188	0 220	0 235	0 074	0 085	0 082
Fe^{2+}	1 840	2 096	2 016	2 063	0 885	0 830	0 857	0 565	0 650	0 732	0 549	0 650	0 503	0 692	0 576	0 737	0 674	0 762
Mn	0 032	0 036	0 039	0 036	0 000	0 000	0 000	0 005	0 001	0 001	0 006	0 004	0 006	0 000	0 000	0 003	0 002	0 002
Ni	0 000	0 000	0 000	0 000	0 000	0 000	0 000	0 000	0 000	0 000	0 000	0 000	0 000	0 000	0 000	0 000	0 000	0 000
Mg	0 927	0 712	0 722	0 722	2 911	2 929	2 923	2 968	2 919	2 942	3 001	2 971	3 066	2 949	2 955	2 816	2 898	2 823
Ca	0 198	0 174	0 202	0 206	0 003	0 002	0 002	0 005	0 005	0 000	0 000	0 000	0 001	0 003	0 006	0 000	0 001	0 003
Na	0 002	0 003	0 003	0 001	0 006	0 000	0 000	0 000	0 000	0 000	0 000	0 000	0 000	0 003	0 000	0 002	0 000	0 002
K	0 000	0 000	0 000	0 000	0 000	0 000	0 000	0 000	0 000	0 000	0 000	0 000	0 000	0 000	0 000	0 000	0 000	0 000
P	0 000	0 002	0 002	0 003	0 002	0 002	0 000	0 001	0 001	0 000	0 000	0 001	0 000	0 000	0 000	0 000	0 004	0 000
Ba	-	-	-	-	-	-	-	-	-	-	-	-	-	-	-	-	-	-
Zn	-	-	-	-	-	-	-	-	-	-	-	-	-	-	-	-	-	-
Total	8 003	8 008	7 996	8 013	14 003	13 999	13 996	13 993	14 010	13 998	13 986	14 003	14 007	14 024	14 015	14 021	14 024	14 010
X_{Mg}	0 34	0 25	0 26	0 26	0 77	0 78	0 77	0 84	0 82	0 80	0 85	0 82	0 86	0 81	0 84	0 79	0 81	0 79
Prp	30 94	23 59	24 23	23 86	-	-	-	-	-	-	-	-	-	-	-	-	-	-
Alm	61 41	69 45	67 67	68 15	-	-	-	-	-	-	-	-	-	-	-	-	-	-
Sps	1 05	1 19	1 32	1 18	-	-	-	-	-	-	-	-	-	-	-	-	-	-
Grs	6 60	5 77	6 78	6 81	-	-	-	-	-	-	-	-	-	-	-	-	-	-

*=Total Fe as FeO n d not detarmined Fe^{3+} is calculated based on stoichiometry

Table 1 Continued

mineral	Plagioclase (O=8)																	
rock type	Grt-felsic gn		Type-A				Type-B						Type-C		Opx-felsic gn			
sample	9812290202		9812280101				9812290501		9812290503	9812290507S			9812290101		9812290801S	9812291002S		
SiO_2	61 52	61 15	54 55	55 67	48 30	56 48	56 65	56 97	59 90	58 47	58 69	58 97	60 22	61 49	58 49	58 36	57 28	58 07
TiO_2	0 12	0 00	0 02	0 00	0 01	0 04	0 00	0 00	0 02	0 06	0 02	0 00	0 00	0 01	0 00	0 00	0 02	0 02
Al_2O_3	24 09	24 74	29 04	28 85	33 05	28 97	27 34	27 05	26 13	26 46	25 77	25 48	24 81	24 27	25 92	26 38	26 51	26 31
Y_2O_3	n d	n d	n d	n d	n d	n d	n d	n d	n d	n d	n d	n d	n d	n d	n d	n d	n d	n d
Yb_2O_3	n d	n d	n d	n d	n d	n d	n d	n d	n d	n d	n d	n d	n d	n d	n d	n d	n d	n d
Cr_2O_3	0 04	0 01	0 00	0 00	0 01	0 00	0 06	0 04	0 00	0 02	0 04	0 00	0 01	0 00	0 01	0 00	0 00	0 02
FeO*	0 01	0 14	0 16	0 00	0 11	0 01	0 31	0 28	0 00	0 37	0 06	0 00	0 16	0 02	0 05	0 05	0 08	0 09
MnO	0 01	0 02	0 00	0 00	0 03	0 03	0 00	0 00	0 02	0 00	0 00	0 02	0 02	0 00	0 00	0 00	0 00	0 01
NiO	0 00	0 01	0 00	0 00	0 00	0 00	0 00	0 00	0 00	0 00	0 00	0 03	0 02	0 04	0 00	0 06	0 05	0 00
MgO	0 00	0 03	0 03	0 00	0 00	0 01	0 02	0 00	0 01	0 00	0 07	0 00	0 00	0 00	0 00	0 01	0 01	0 02
CaO	5 90	6 35	11 46	11 19	16 38	10 69	9 34	9 65	7 84	8 25	8 03	7 62	6 58	6 04	8 06	8 08	8 52	8 26
Na_2O	8 21	7 97	4 95	5 17	2 30	5 61	6 13	6 12	7 26	6 69	7 00	7 19	7 67	8 03	6 87	6 86	6 55	6 71
K_2O	0 17	0 26	0 09	0 12	0 03	0 09	0 14	0 10	0 16	0 10	0 18	0 19	0 22	0 24	0 29	0 20	0 22	0 20
P_2O_5	0 02	0 00	0 02	0 00	0 00	0 01	0 00	0 02	0 05	0 01	0 04	0 02	0 00	0 00	0 14	0 02	0 04	0 04
BaO	0 00	0 00	n d	n d	n d	n d	n d	n d	n d	n d	0 05	0 01	0 00	0 06	0 00	0 01	0 01	0 00
ZnO	n d	n d	n d	n d	n d	n d	n d	n d	n d	n d	n d	n d	n d	n d	n d	n d	n d	n d
Total	100 09	100 68	100 32	101 00	100 22	101 94	99 99	100 24	101 38	100 45	99 93	99 51	99 71	100 19	99 83	100 03	99 30	99 73
Si	2 730	2 704	2 454	2 482	2 208	2 493	2 546	2 554	2 637	2 605	2 627	2 646	2 690	2 727	2 619	2 609	2 585	2 605
Ti	0 004	0 000	0 001	0 000	0 000	0 001	0 000	0 000	0 001	0 002	0 001	0 000	0 000	0 000	0 000	0 000	0 001	0 001
Al	1 260	1 289	1 540	1 516	1 781	1 507	1 448	1 429	1 356	1 389	1 359	1 347	1 306	1 269	1 368	1 390	1 410	1 391
Fe^{3+}	-	-	-	-	-	-	-	-	-	-	-	-	-	-	-	-	-	-
Y	-	-	-	-	-	-	-	-	-	-	-	-	-	-	-	-	-	-
Yb	-	-	-	-	-	-	-	-	-	-	-	-	-	-	-	-	-	-
Cr	0 001	0 000	0 000	0 000	0 000	0 000	0 002	0 002	0 000	0 001	0 001	0 000	0 000	0 000	0 000	0 000	0 000	0 001
Fe^{2+}	0 000	0 005	0 006	0 000	0 004	0 000	0 012	0 010	0 000	0 014	0 002	0 000	0 006	0 001	0 002	0 002	0 003	0 003
Mn	0 000	0 001	0 000	0 000	0 001	0 001	0 000	0 000	0 001	0 000	0 000	0 001	0 001	0 000	0 000	0 000	0 000	0 000
Ni	0 000	0 000	0 000	0 000	0 000	0 000	0 000	0 000	0 000	0 000	0 000	0 001	0 001	0 001	0 000	0 002	0 002	0 000
Mg	0 000	0 002	0 002	0 000	0 000	0 001	0 002	0 000	0 001	0 000	0 005	0 000	0 000	0 000	0 000	0 001	0 001	0 001
Ca	0 280	0 301	0 552	0 535	0 802	0 505	0 450	0 464	0 370	0 394	0 385	0 366	0 315	0 287	0 387	0 387	0 412	0 397
Na	0 707	0 683	0 432	0 447	0 204	0 480	0 534	0 532	0 620	0 578	0 608	0 625	0 664	0 690	0 597	0 595	0 573	0 584
K	0 010	0 015	0 005	0 007	0 002	0 005	0 008	0 006	0 009	0 006	0 010	0 011	0 013	0 013	0 017	0 012	0 013	0 011
P	0 001	0 000	0 001	0 000	0 000	0 000	0 000	0 001	0 002	0 000	0 001	0 001	0 000	0 000	0 005	0 001	0 002	0 001
Ba	0 000	0 000	-	-	-	-	-	-	-	-	0 001	0 000	0 000	0 001	0 000	0 000	0 000	0 000
Zn	-	-	-	-	-	-	-	-	-	-	-	-	-	-	-	-	-	-
Total	4 993	5 000	4 993	4 987	5 003	4 994	5 001	4 998	4 996	4 990	4 999	4 998	4 995	4 990	4 995	4 998	5 000	4 995
Ab	70 91	68 40	43 65	45 24	20 24	48 46	53 85	53 11	62 06	59 11	60 60	62 39	66 96	69 69	59 67	59 90	57 45	58 84
An	28 13	30 14	55 82	54 09	79 61	51 03	45 34	46 30	37 02	40 29	38 39	36 52	31 77	28 96	38 68	38 94	41 26	40 02
Or	0 96	1 46	0 53	0 67	0 15	0 50	0 81	0 59	0 91	0 60	1 01	1 09	1 28	1 35	1 66	1 17	1 29	1 14

*=Total Fe as FeO n d not determined

Table 1 Continued.

mineral	Or lamella in Mesoperthite (O=8)																	
rock type	Grt-felsic gn			Type-A			Type-B							Type-C			Opx-felsic gn	
sample	9812290202			9812280101			9812290507S							9812290101			9812290801S	9812291002S
SiO_2	65 16	64 59	64 94	64 63	63 45	64 24	64 51	64 29	63 67	63 54	64 26	64 33	64 34	65 12	64 68	64 79	64 04	64 13	63 70
TiO_2	0 08	1 07	0 15	0 12	0 11	0 12	0 09	0 06	0 10	0 15	0 06	0 05	0 06	0 08	0 06	0 03	0 05	0 04	0 09
Al_2O_3	18 28	18 20	18 44	18 76	18 88	18 84	18 42	18 59	18 20	18 32	18 82	18 40	18 40	18 54	18 51	18 51	18 65	18 60	18 44
Y_2O_3	n d	n d	n d	n d	n d	n d	n d	n d	n d	n d	n d	n d	n d	n d	n d	n d	n d	n d	n d
Yb_2O_3	n d	n d	n d	n d	n d	n d	n d	n d	n d	n d	n d	n d	n d	n d	n d	n d	n d	n d	n d
Cr_2O_3	0 01	0 05	0 02	0 01	0 00	0 02	0 00	0 03	0 02	0 00	0 00	0 01	0 00	0 00	0 02	0 02	0 05	0 03	0 00
FeO*	0 00	0 05	0 01	0 00	0 03	0 04	0 00	0 01	0 00	0 05	0 00	0 00	0 02	0 03	0 00	0 02	0 00	0 02	0 02
MnO	0 01	0 00	0 00	0 00	0 00	0 01	0 00	0 01	0 00	0 00	0 03	0 01	0 00	0 03	0 03	0 02	0 01	0 00	0 01
NiO	0 00	0 05	0 00	0 00	0 03	0 02	0 00	0 00	0 03	0 01	0 07	0 00	0 00	0 02	0 01	0 00	0 03	0 02	0 00
MgO	0 00	0 00	0 00	0 00	0 02	0 00	0 00	0 00	0 00	0 00	0 01	0 00	0 00	0 01	0 00	0 01	0 00	0 00	0 00
CaO	0 06	0 07	0 11	0 10	0 06	0 14	0 08	0 04	0 02	0 01	0 21	0 05	0 11	0 07	0 10	0 10	0 05	0 09	0 08
Na_2O	1 09	1 15	1 25	1 15	1 19	1 41	1 08	1 15	1 40	1 19	0 80	0 95	0 91	0 84	1 07	1 45	0 64	0 74	0 83
K_2O	15 30	15 02	15 06	14 28	14 49	13 75	14 96	14 50	14 40	14 53	15 28	15 26	15 37	15 04	15 15	15 00	15 66	15 50	15 10
P_2O_5	0 05	0 05	0 00	0 03	0 00	0 06	0 00	0 01	0 01	0 01	0 01	0 00	0 01	0 03	0 00	0 01	0 04	0 10	0 05
BaO	0 58	0 62	0 41	1 55	2 61	2 27	1 03	1 13	2 17	2 54	0 84	0 72	0 78	0 77	0 71	0 70	1 25	1 01	1 00
ZnO	n d	n d	n d	n d	n d	n d	n d	n d	n d	n d	n d	n d	n d	n d	n d	n d	n d	n d	n d
Total	100 63	100 92	100 39	100 64	100 89	100 91	100 18	99 81	100 02	100 35	100 38	99 78	10000	100 58	100 34	100 66	100 48	100 26	99 31
Si	2 996	2 966	2 989	2 978	2 951	2 965	2 987	2 983	2 976	2 969	2 970	2 987	2 985	2 993	2 985	2 982	2 971	2 973	2 977
Ti	0 003	0 037	0 005	0 004	0 004	0 004	0 003	0 002	0 003	0 005	0 002	0 002	0 002	0 003	0 002	0 001	0 002	0 001	0 003
Al	0 991	0 985	1 000	1 019	1 035	1 025	1 005	1 016	1 003	1 009	1 025	1 007	1 006	1 004	1 007	1 004	1 019	1 016	1 016
Fe^{3+}	-	-	-	-	-	-	-	-	-	-	-	-	-	-	-	-	-	-	-
Y	-	-	-	-	-	-	-	-	-	-	-	-	-	-	-	-	-	-	-
Yb	-	-	-	-	-	-	-	-	-	-	-	-	-	-	-	-	-	-	-
Cr	0 000	0 002	0 001	0 000	0 000	0 001	0 000	0 001	0 001	0 000	0 000	0 001	0 000	0 000	0 001	0 001	0 002	0 001	0 000
Fe^{2+}	0 000	0 002	0 000	0 000	0 001	0 001	0 000	0 001	0 000	0 002	0 000	0 000	0 001	0 001	0 000	0 001	0 000	0 001	0 001
Mn	0 001	0 000	0 000	0 000	0 000	0 000	0 000	0 000	0 000	0 000	0 001	0 000	0 000	0 001	0 001	0 001	0 000	0 000	0 000
Ni	0 000	0 002	0 000	0 000	0 001	0 001	0 000	0 000	0 001	0 000	0 003	0 000	0 000	0 001	0 000	0 000	0 001	0 001	0 000
Mg	0 000	0 000	0 000	0 000	0 001	0 000	0 000	0 000	0 000	0 000	0 001	0 000	0 000	0 001	0 000	0 001	0 000	0 000	0 000
Ca	0 003	0 003	0 005	0 005	0 003	0 007	0 004	0 002	0 001	0 000	0 010	0 003	0 006	0 003	0 005	0 005	0 002	0 004	0 004
Na	0 097	0 103	0 112	0 103	0 107	0 126	0 097	0 103	0 127	0 108	0 072	0 086	0 082	0 075	0 096	0 129	0 058	0 066	0 075
K	0 897	0 880	0 884	0 840	0 860	0 809	0 884	0 858	0 859	0 866	0 901	0 904	0 909	0 882	0 892	0 881	0 927	0 917	0 900
P	0 002	0 002	0 000	0 001	0 000	0 002	0 000	0 001	0 000	0 000	0 001	0 000	0 000	0 001	0 000	0 001	0 002	0 004	0 002
Ba	0 010	0 011	0 007	0 028	0 048	0 041	0 019	0 021	0 040	0 047	0 015	0 013	0 014	0 014	0 013	0 013	0 023	0 018	0 018
Zn	-	-	-	-	-	-	-	-	-	-	-	-	-	-	-	-	-	-	-
Total	5 000	4 992	5 004	4 978	5 011	4 983	4 998	4 987	5 011	5 007	5 000	5 002	5 005	4 979	5 003	5 018	5 007	5 002	4 997
Ab	9 75	10 41	11 15	10 86	11 08	13 40	9 88	10 72	12 85	11 05	7 30	8 65	8 21	7 81	9 68	12 74	5 87	6 70	7 66
An	0 29	0 33	0 52	0 54	0 28	0 75	0 39	0 20	0 09	0 04	1 05	0 27	0 56	0 34	0 51	0 49	0 25	0 43	0 43
Or	89 96	89 26	88 33	88 60	88 64	85 85	89 73	89 09	87 06	88 91	91 65	91 08	91 24	91 85	89 81	86 77	93 88	92 86	91 91

*=Total Fe as FeO n d not detarmined

Table 1 Continued

mineral	Orthopyroxene (O=6)								Spinel (O=4)					Cordierite (O=18)	
rock type	Type-B				Opx-felsic gn				Type-A			Type-B		Type-B	
sample	9812290501	9812290507S			9812290801S				9812280101			9812290503		9812290501	
SiO_2	52 37	52 08	50 46	51 27	50 28	49 22	48 01	49 68	0 14	0 02	0 01	0 00	0 01	50 61	50 11
TiO_2	0 07	0 07	0 09	0 10	0 03	0 07	0 06	0 05	0 00	0 00	0 01	0 00	0 01	0 02	0 00
Al_2O_3	6 19	6 26	8 03	6 79	3 67	4 81	5 22	4 37	61 00	60 69	59 74	59 98	59 69	33 56	33 70
Y_2O_3	n d	n d	n d	n d	n d	n d	n d	n d	n d	n d	n d	n d	n d	n d	n d
Yb_2O_3	n d	n d	n d	n d	n d	n d	n d	n d	n d	n d	n d	n d	n d	n d	n d
Cr_2O_3	0 25	0 22	0 32	0 23	0 01	0 01	0 05	0 05	4 15	3 91	4 39	4 93	5 17	0 00	0 02
FeO*	13 04	13 34	14 38	14 16	28 02	26 55	28 61	25 35	16 61	20 75	18 88	17 09	17 20	2 06	1 79
MnO	0 04	0 02	0 09	0 06	0 14	0 25	0 16	0 13	0 08	0 03	0 03	0 05	0 03	0 01	0 00
NiO	0 00	0 00	0 00	0 00	0 00	0 00	0 00	0 00	0 24	0 22	0 16	0 13	0 13	0 00	0 00
MgO	28 47	27 73	26 33	26 76	18 52	18 29	17 31	19 63	15 41	12 95	13 98	14 77	14 45	12 48	12 38
CaO	0 03	0 07	0 06	0 09	0 16	0 15	0 23	0 19	0 00	0 00	0 01	0 00	0 00	0 09	0 02
Na_2O	0 00	0 00	0 00	0 00	0 01	0 00	0 00	0 00	0 00	0 00	0 00	0 00	0 00	0 05	0 04
K_2O	0 00	0 00	0 22	0 00	0 00	0 00	0 00	0 00	0 00	0 00	0 00	0 00	0 00	0 01	0 00
P_2O_5	0 00	0 00	0 00	0 00	0 01	0 00	0 03	0 00	0 00	0 00	0 00	0 00	0 01	0 00	0 03
BaO	n d	n d	n d	n d	n d	n d	n d	n d	n d	n d	n d	n d	n d	n d	n d
ZnO	n d	n d	n d	n d	n d	n d	n d	n d	2 07	2 16	2 03	3 55	3 32	n d	n d
Total	100 44	99 80	99 97	99 46	100 85	99 34	99 66	99 44	99 69	100 72	99 23	100 50	100 01	98 88	98 09
Si	1 854	1 858	1 811	1 844	1 904	1 882	1 852	1 887	0 004	0 000	0 000	0 000	0 000	5 031	5 014
Ti	0 002	0 002	0 002	0 003	0 001	0 002	0 002	0 001	0 000	0 000	0 000	0 000	0 000	0 001	0 000
Al	0 258	0 263	0 339	0 288	0 164	0 217	0 237	0 196	1 896	1 902	1 888	1 873	1 874	3 932	3 974
Fe^{3+}	-	-	-	-	-	-	-	-	-	-	-	-	-	-	-
Y	-	-	-	-	-	-	-	-	-	-	-	-	-	-	-
Yb	-	-	-	-	-	-	-	-	-	-	-	-	-	-	-
Cr	0 007	0 006	0 009	0 007	0 000	0 000	0 001	0 001	0 086	0 082	0 093	0 103	0 109	0 000	0 001
Fe^{2+}	0 386	0 398	0 432	0 426	0 887	0 849	0 923	0 805	0 366	0 462	0 424	0 379	0 383	0 171	0 149
Mn	0 001	0 001	0 003	0 002	0 005	0 008	0 005	0 004	0 002	0 001	0 001	0 001	0 001	0 000	0 000
Ni	0 000	0 000	0 000	0 000	0 000	0 000	0 000	0 000	0 005	0 005	0 003	0 003	0 003	0 000	0 000
Mg	1 503	1 475	1 409	1 435	1 045	1 043	0 995	1 111	0 606	0 514	0 559	0 583	0 574	1 850	1 847
Ca	0 001	0 002	0 002	0 004	0 007	0 006	0 009	0 008	0 000	0 000	0 000	0 000	0 000	0 009	0 002
Na	0 000	0 000	0 000	0 000	0 001	0 000	0 000	0 000	0 000	0 000	0 000	0 000	0 000	0 010	0 008
K	0 000	0 000	0 010	0 000	0 000	0 000	0 000	0 000	0 000	0 000	0 000	0 000	0 000	0 001	0 000
P	0 000	0 000	0 000	0 000	0 000	0 000	0 001	0 000	0 000	0 000	0 000	0 000	0 000	0 000	0 003
Ba	-	-	-	-	-	-	-	-	-	-	-	-	-	-	-
Zn	-	-	-	-	-	-	-	-	0 040	0 042	0 040	0 070	0 065	-	-
Total	4 012	4 006	4 017	4 007	4 013	4 007	4 026	4 014	3 005	3 007	3 009	3 012	3 008	11 007	10 999
X_{Mg}	0 80	0 79	0 77	0 77	0 54	0 55	0 52	0 58	0 623	0 527	0 569	0 606	0 600	0 92	0 93
En	79 52	78 64	76 46	76 97	53 90	54 93	51 63	57 75	-	-	-	-	-	-	-
Fs	20 43	21 22	23 42	22 85	45 76	44 74	47 88	41 84	-	-	-	-	-	-	-
Wo	0 05	0 13	0 12	0 19	0 34	0 32	0 49	0 41	-	-	-	-	-	-	-

*=Total Fe as FeO n d not detarmined

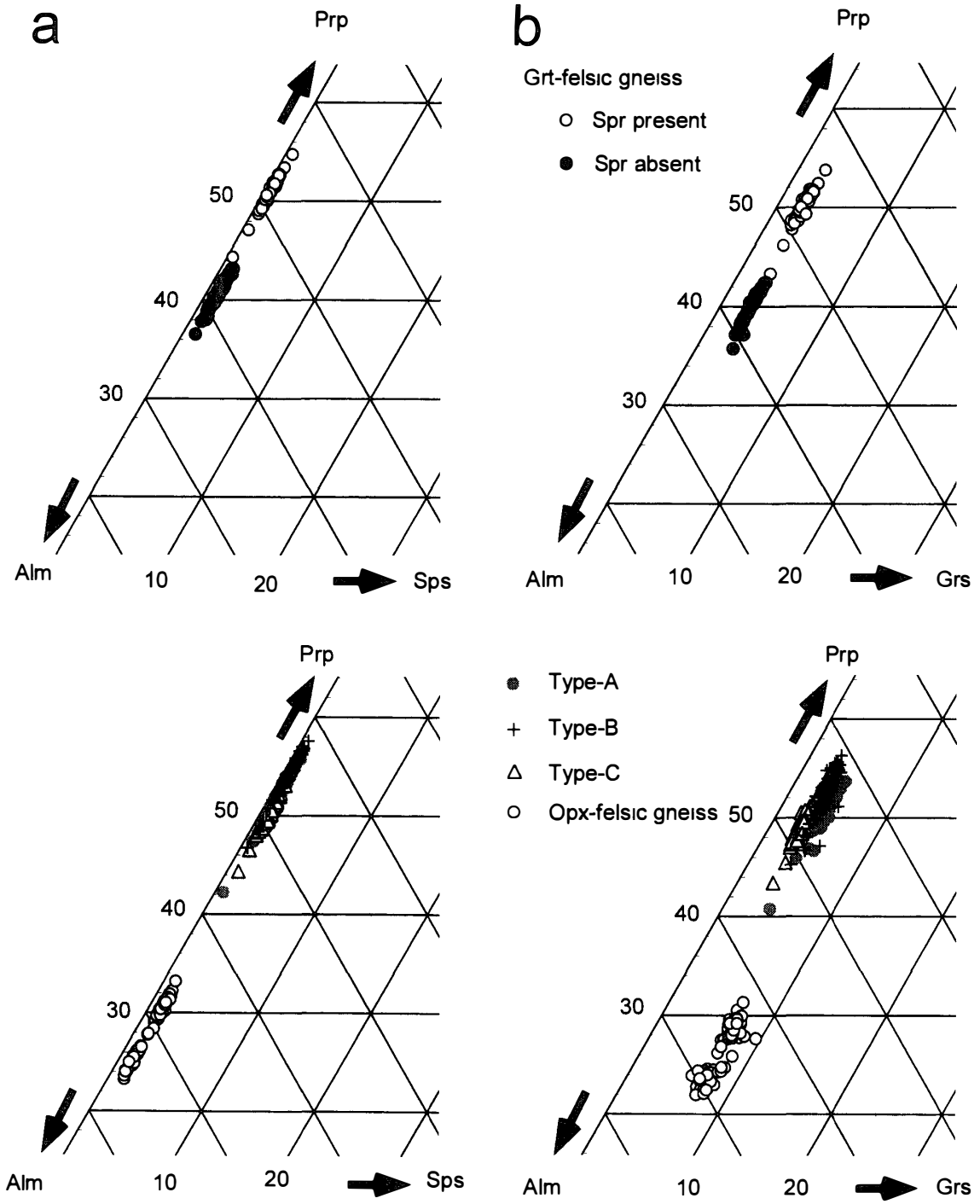

Fig 9 (a) Pyrope (Prp)-almandine (Alm)-spessartine (Sps) diagram of garnet compositions of rocks from Howard Hills (b) Pyrope (Prp)-almandine (Alm)-grossular (Grs) diagram of garnet compositions of rocks from Howard Hills

of coarsely crystalline garnets with quartz inclusions in the type-A aluminous gneiss reaches relatively highly maximum values (about 0 15 wt%) than those of finely crystalline garnets in the type-A aluminous gneisses and those of the other rock types, which contain about 0 1 wt% (Fig 11)

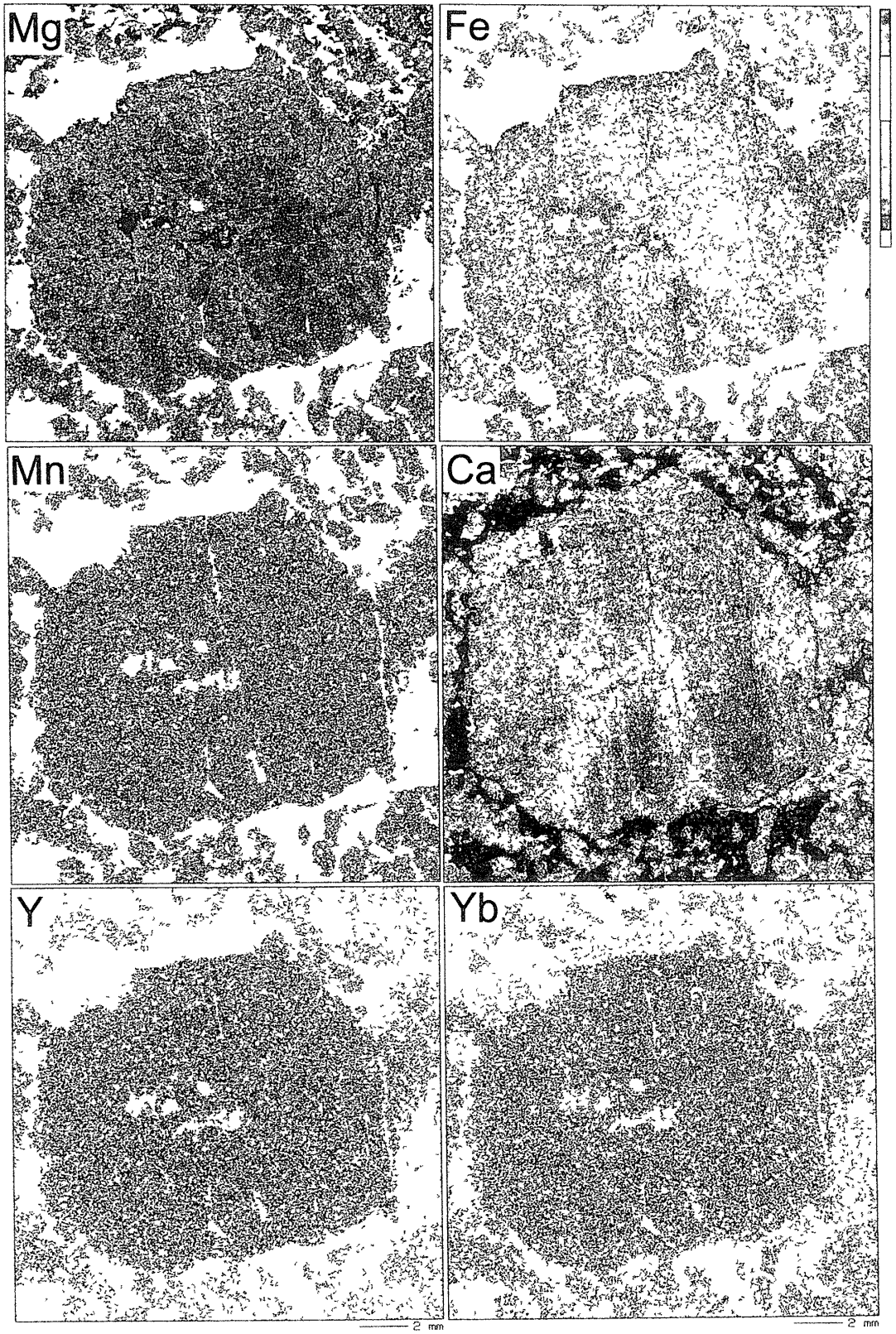

Fig 10a

Fig 10 Two-dimensional compositional maps of garnet (a) Type-A aluminous gneiss (b) Type-B aluminous gneiss

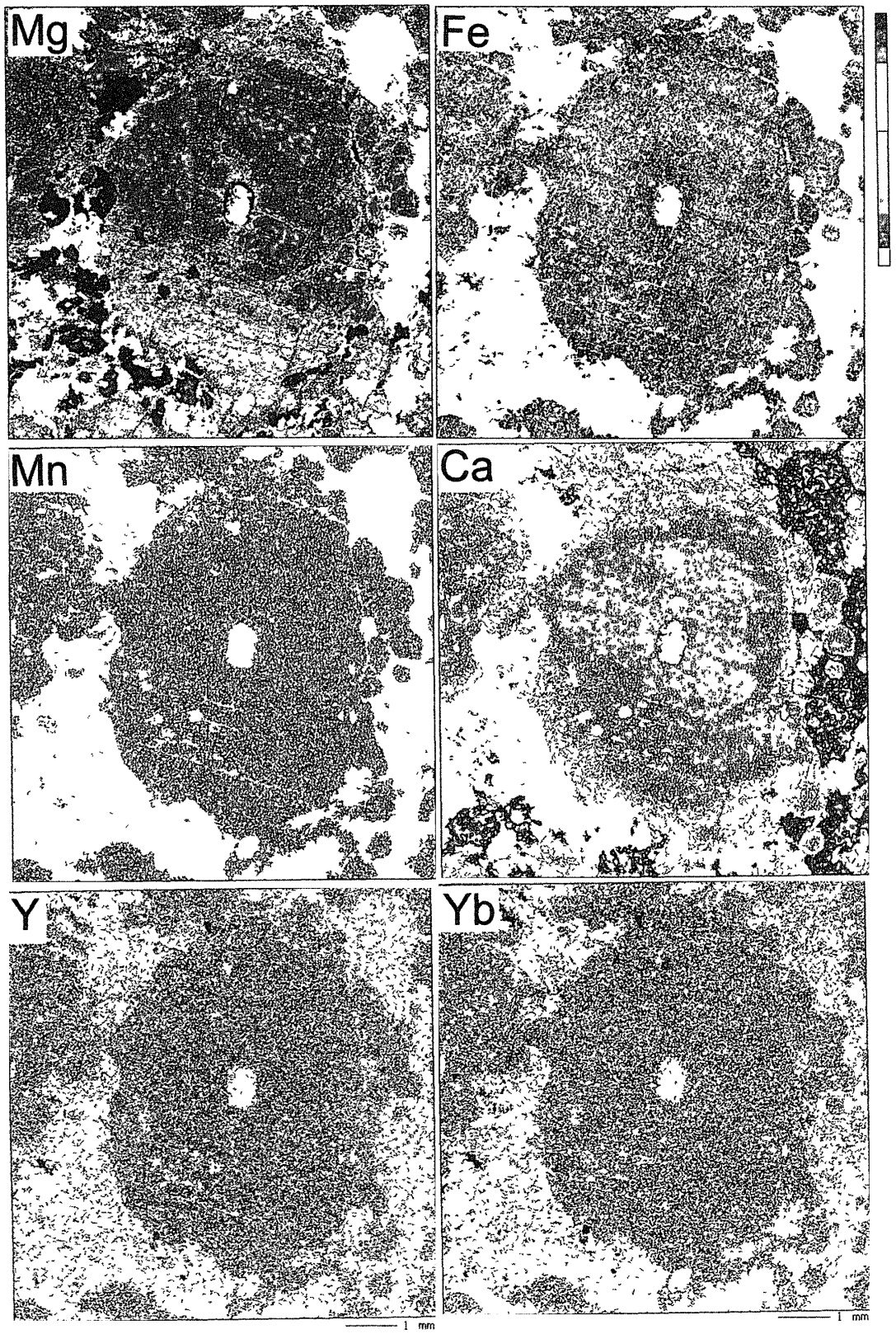

Fig 10b

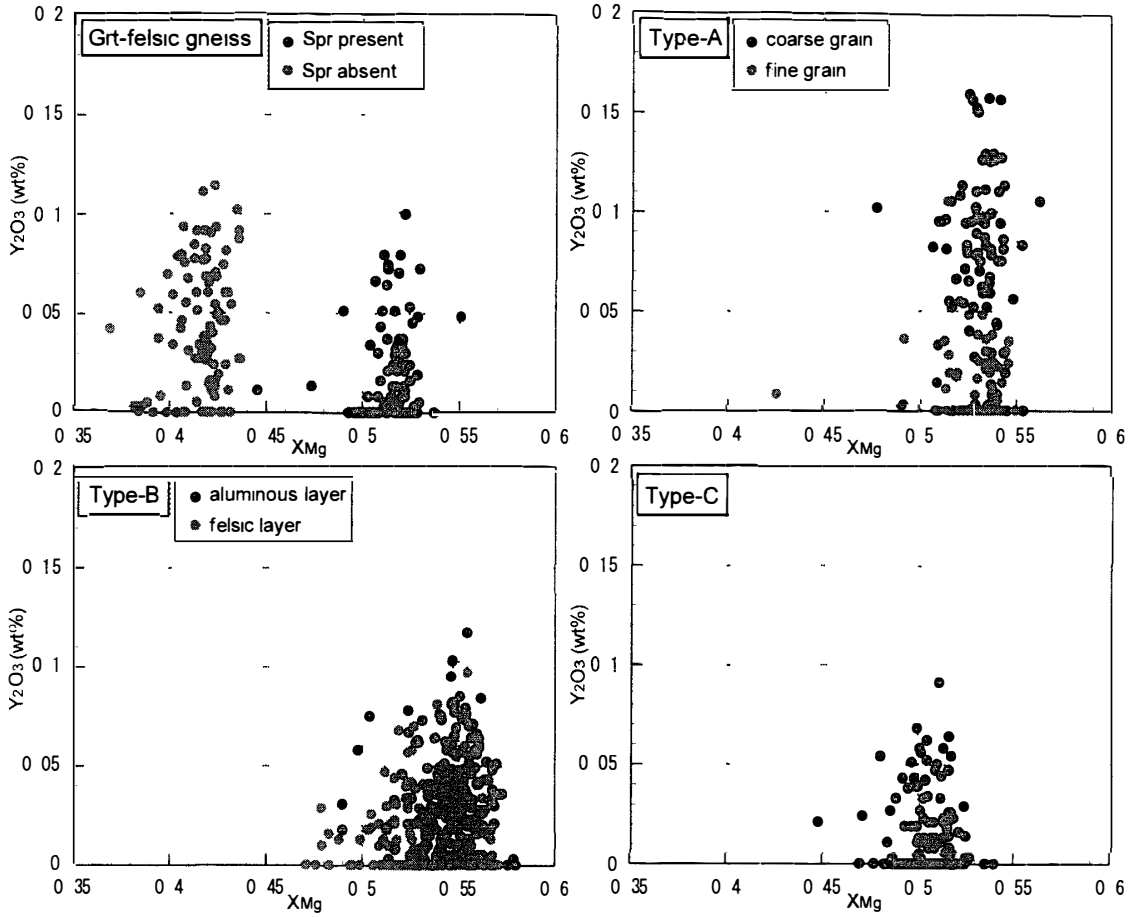

Fig 11 Variation of Y and X_{Mg} contents of garnets from garnet felsic gneiss and aluminous gneiss

3 2 2 Sapphirine

The X_{Mg} (Mg/[Mg+Fe])-Cr_2O_3 plot for sapphirine is shown in Fig 12 X_{Mg} of sapphirine in types-A and -B aluminous gneisses ranges from 0 77 to 0 86, and those from the garnet felsic gneiss and type-C aluminous gneiss range from 0 73 to 0 82 Sapphirines from all rock types contain some Cr_2O_3 the sapphirine from the aluminous layer of the type-B aluminous gneiss contains about 0 9–2 5 wt% Cr_2O_3, and the sapphirine coexisting with quartz in the felsic layer of the type-B aluminous gneiss contains about 2 2–2 7 wt% Cr_2O_3 The sapphirine in the garnet felsic gneiss and the acicular sapphirine from the type-C aluminous gneiss contain about 1–1 5 wt% and about 0 6–1 wt% Cr_2O_3, respectively The relation between the X_{Mg} value and Cr_2O_3 content of sapphirine and the included rock types is being examined for samples from Tonagh Island, results thus for are similar to the result at Howard Hills (Osanai, pers communication) Fe^{3+} content for sapphirine was obtained by stoichiometric calculation (O=20) using the method of Higgins *et al* (1979) Fe^{3+} of sapphirine in garnet felsic gneiss and types-A, -B, and -C aluminous gneisses is the maximum of 0 04, 0 14 and 0 1 wt%, respectively, on the basis of O=20

3 2 3 Plagioclase

The An and Or contents of plagioclase are shown in Fig 13 The An content is richest (An50–70) in type-A aluminous gneiss Plagioclase compositions are about An30–

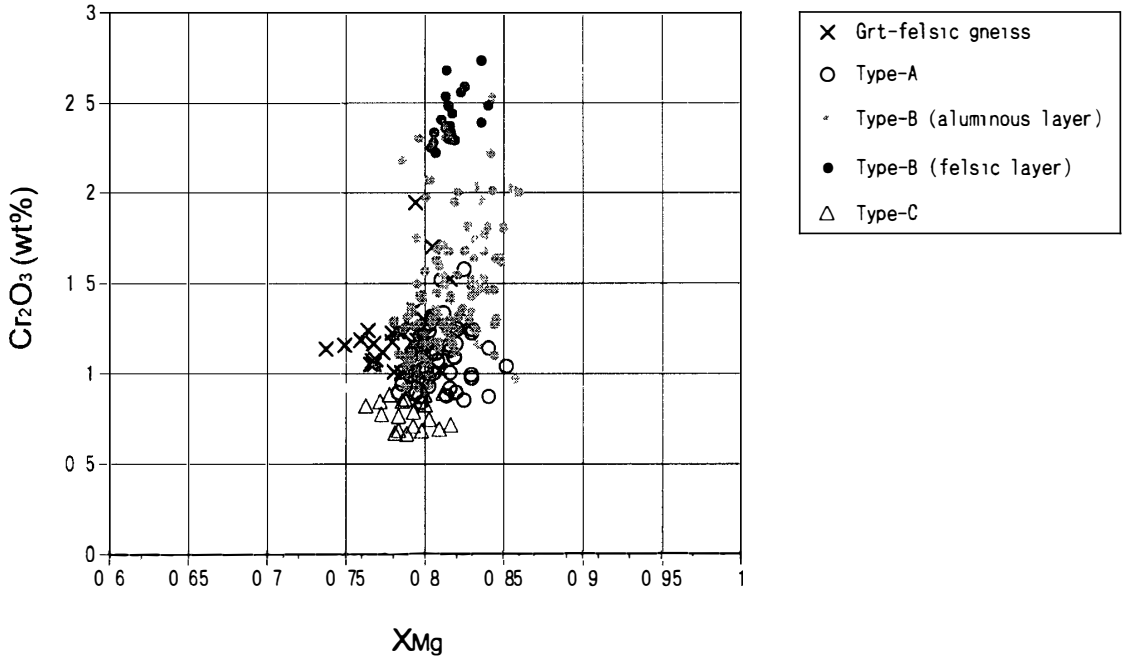

Fig 12 Plot of Cr versus X_{Mg} in sapphirine for garnet felsic gneiss and aluminous gneiss Fe^{2+} and Fe^{3+} of sapphirine were calculated based on stoichiometry (Higgins et al., 1979)

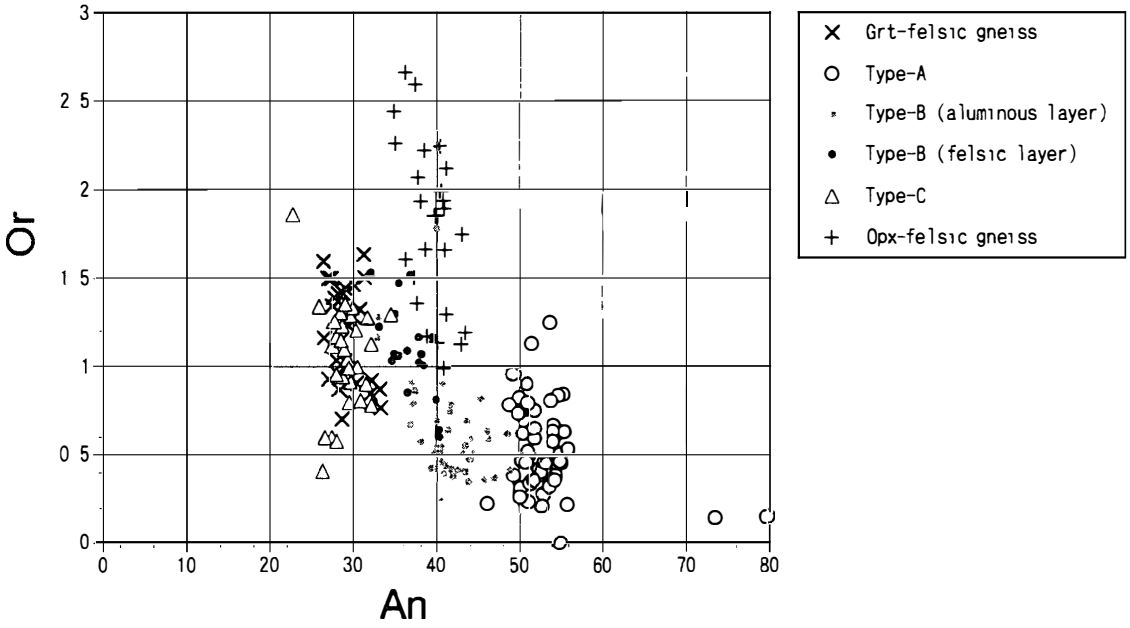

Fig 13 Variations in Or content and An value of plagioclase from garnet felsic gneiss, aluminous gneiss and orthopyroxene felsic gneiss from Howard Hills

45 in type-B aluminous gneiss, and An25-35 in both the garnet felsic gneiss and type-C aluminous gneiss Type-B aluminous gneisses have high An and low Or in the aluminous layer, and low An and high Or content in the quartzo-feldspathic layer. Orthopyroxene felsic gneiss has a value of An33-44; it is richer in Or than other rock types

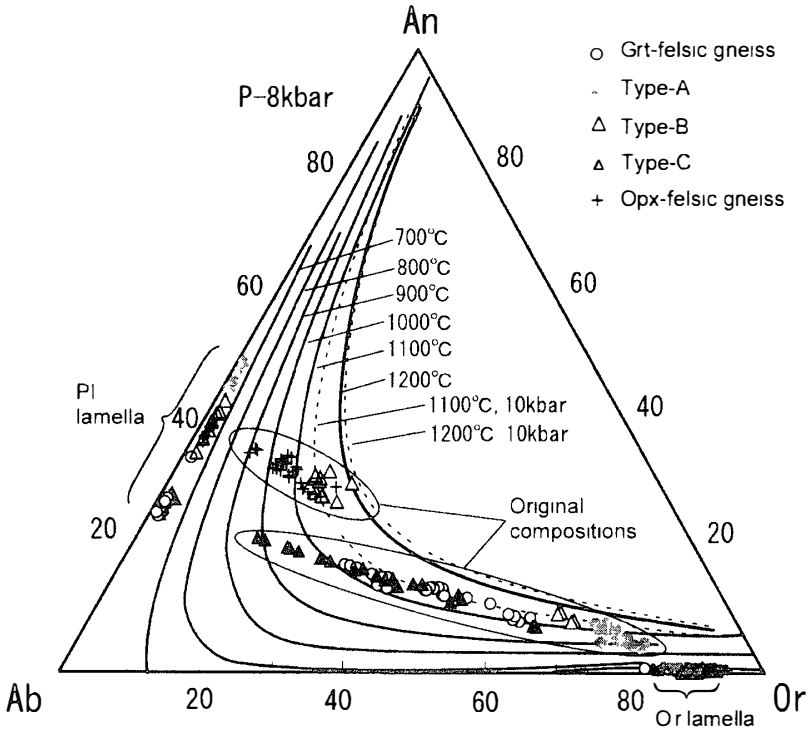

Fig 14 An-Ab-Or ternary feldspar diagram of calculated original alkali-feldspar composition, from plagioclase and orthoclase lamella compositions in samples from Howard Hills Ternary miscibility gaps are calculated for P = 8 kbar (solid line) and P = 10 kbar (broken line) using the method of Kroll et al (1993)

3 2 4 Mesoperthite

The original chemical compositions of mesoperthite from garnet felsic gneiss, aluminous gneiss and orthopyroxene felsic gneiss were obtained using the modal ratio of host and lamella and their respective chemical compositions The restoration method used the following procedures

1) A BEI photograph was taken for the mesoperthite
2) The BEI image was scanned into a personal computer
3) The image was loaded into image-analyzing software (*e.g* PhotoShop), and the modal ratio of each type of mesoperthite lamella was obtained using the binarization function (Or lamellae appear white, and Ab lamellae appear black in a BEI image)
4) The original composition of alkali feldspar was calculated by using the modal ratio of each lamella obtained in (3) and the compositions of the two lamella types obtained by EPMA

Although the plagioclase and K-feldspar lamellae re-equilibrated chemically at low temperature, the chemical composition obtained by this method indicates the chemical composition of the initial, very high-temperature, pre-exsolution feldspar (Fig 14) Temperature estimation is discussed below

BaO contents of K-feldspar lamellae in mesoperthite vary with rock type Garnet felsic gneiss and type-C aluminous gneiss have low BaO values (0 4–0 8 wt%), whereas type-A and -B aluminous gneisses have high values (maximum 2 7 wt%) The BaO contents of type-A and -B aluminous gneisses fall into two domains 2–2 7 wt% and 1–1 6

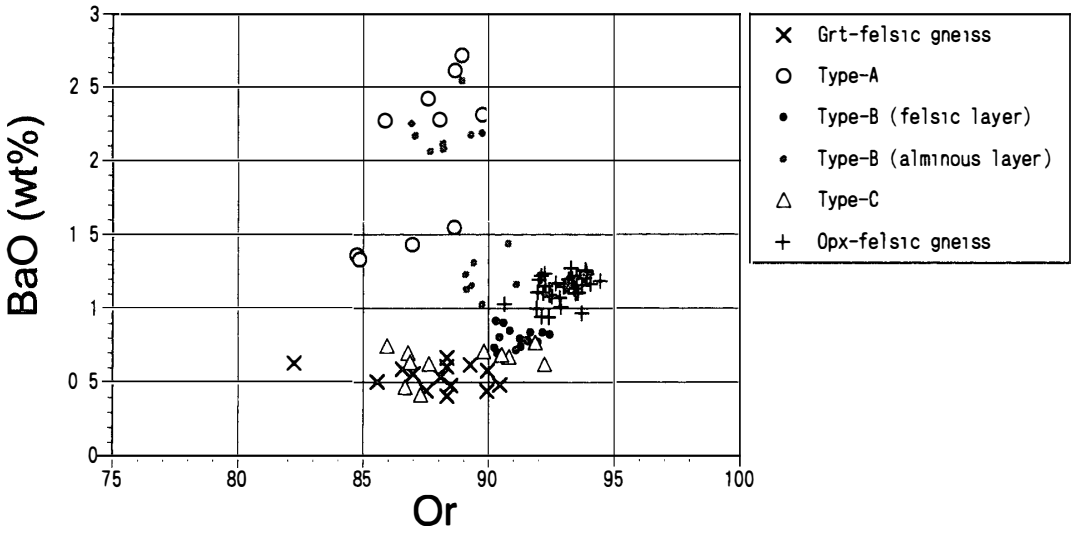

Fig 15 Compositional variation of Or-lamella or host in perthite to mesoperthite in the rocks from Howard Hills

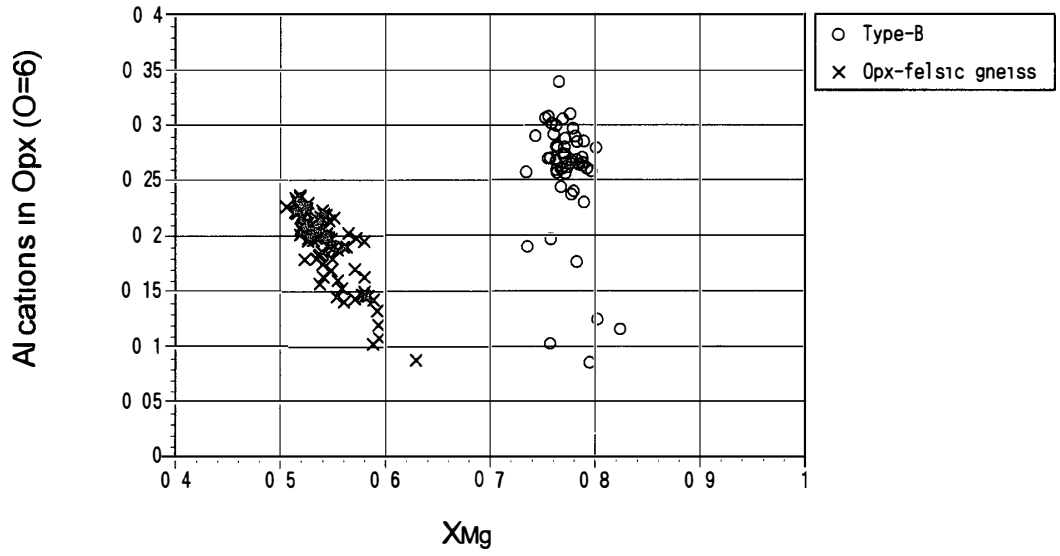

Fig 16 Variations in Al content (per 6-oxygen formula unit) and X_{Mg} of orthopyroxene in type-B aluminous gneiss and orthopyroxene felsic gneiss from Howard Hills

wt% BaO contents of K-feldspar lamella within mesoperthite in orthopyroxene felsic gneiss are 0 9–1 3 wt% (Fig 15)

3 2 5 Orthopyroxene

Orthopyroxene is present in the orthopyroxene felsic gneiss and, rarely, in the aluminous layers of type-B aluminous gneiss In the orthopyroxene felsic gneiss, X_{Mg} and Al_2O_3 contents are 0 51–0.58 and 3 5–5 1 wt%, respectively Orthopyroxene generally shows compositional zoning, with Al values highest in the core and gradually decreasing toward the rim (Fig 16) X_{Mg} is lowest in the core, and increases toward the rim X_{Mg} and Al_2O_3 content of orthopyroxene in type-B aluminous gneiss ranges from 0 74 to 0 8 and from 6 to 8 wt%, respectively Orthopyroxenes of the type-B aluminous gneiss have high

Al content in the core that decreases toward the rim, and slightly higher X_{Mg} in the rim than in the core

3 2 6 Spinel

Spinel is brown under the plane-polarized light in all rock types Spinel analyses were performed on type-A and type-B aluminous gneisses Cr_2O_3 and ZnO contents of spinels in the type-A aluminous gneiss range from 4 to 5 wt% and 1 7 to 2 2 wt%, respectively Spinels from type-B aluminous gneiss contain 4 7–5 5 wt% Cr_2O_3 and 3 4–3 5 wt% ZnO

3 2 7 Cordierite

Cordierite is present only in aluminous layers of type-B aluminous gneiss, where it coexists with sapphirine, orthopyroxene and garnet Cordierite has an X_{Mg} value of 0 9–0 93 wt%

4. Discussion

4 1 Metamorphic conditions

The coexistence of sapphirine and quartz in the Howard Hills gneisses indicates that these rocks have been formed under the stability field of sapphirine + quartz, over 1030°C at 9 5 kbar (Hensen and Green, 1973) or over 1050°C at 11 kbar (Bertrand *et al* , 1991), during peak metamorphism These are minimum conditions, as higher temperatures are plausible, depending on the pressure condition Moreover, the sapphirine + quartz stability field may be shifted in this case, because sapphirine and spinel from the Howard Hills contain Cr and Zn

Hokada *et al* (1999b) showed that An-Ab-Or ternary feldspar solvus is useful in estimating the peak metamorphic temperature of ultrahigh-temperature metamorphic rocks On this basis, it is plausible that the peak metamorphic condition of the Howard Hills garnet felsic, aluminous, and orthopyroxene gneisses could be estimated by applying the ternary feldspar solvus method to the restored chemical compositions of high-temperature feldspars that had undergone retrograde mesoperthitic exsolution The solvus used is that of Kroll *et al* (1993), which is a modified version of that of Elkins and Grove (1990) The peak metamorphic condition is estimated to be about 1000–1200°C at 8 kbar and 1000–1150°C at 10 kbar (Fig 14) All of the gneisses are thus the result of ultrahigh-temperature metamorphism at temperatures of 1000°C or more As a cautionary note, a slight error may be introduced into the calculation when the modal ratio of each lamella is obtained by computer analysis of a BEI mesoperthite image The error trend appears on the line that connects the analysis point of the plagioclase lamella with the analysis point of the orthoclase lamella, when the restored composition is plotted on the ternary solvus The estimated temperature is not affected by the error when the restored original composition is located in the alkali feldspar region, because the error trend is parallel with the solvus line When the composition is plotted in the plagioclase region, the temperature estimate contains some uncertainty because the error trend crosses the solvus line Even when this is taken into consideration, however, the reliability of the temperature estimates for the garnet felsic gneiss, the type-C aluminous gneiss, and some of the type-A and -B aluminous gneisses is high, because the original compositions of mesoperthites in these rocks are located in the alkali-feldspar area

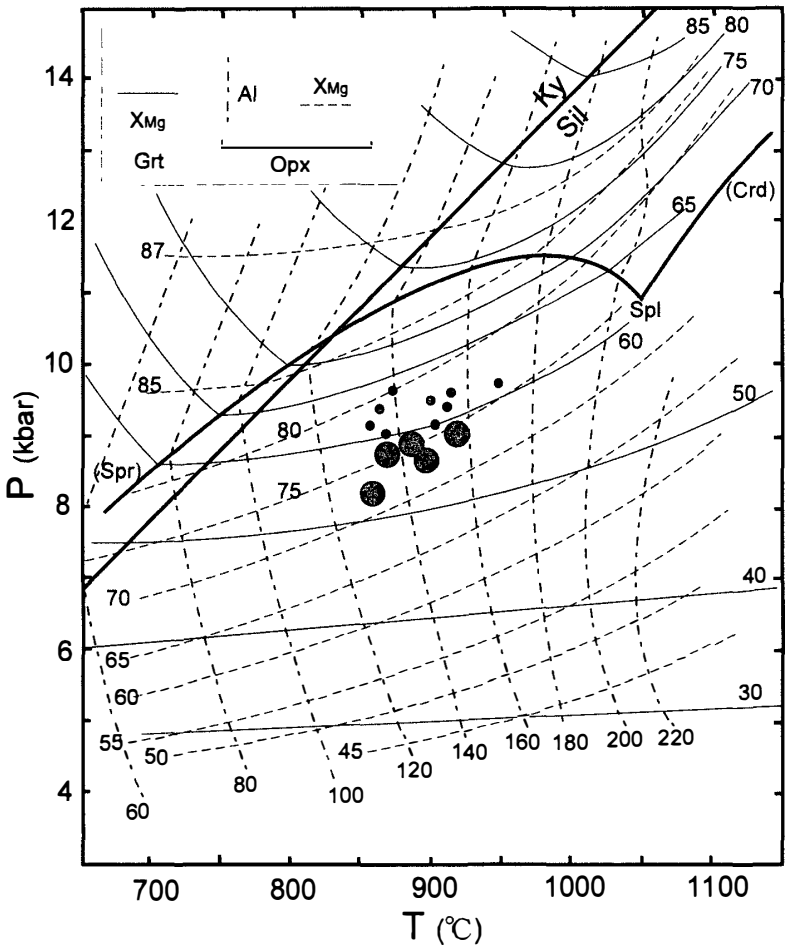

Fig 17 Estimated P and T conditions from X_{Mg} in garnet and X_{Mg} and X_{Al} in orthopyroxene, on X_{Mg} and X_{Al} isopleths of Hensen and Harley (1990) X_{Mg} value of garnet in units $\times 100$ (solid lines) X_{Mg} value of orthopyroxene in units $\times 100$ (dashed line) X_{Al} value of orthopyroxene expressed as units of (Al cations/2, per 6-oxygen units)$\times 1000$ Solid and large circle symbols are equilibrium composition of orthopyroxene and coexisting garnet in type-B aluminous gneiss Solid and small point symbols show the orthopyroxene with disequilibrium composition relative to coexisting garnet.

Hokada *et al* (1999b) estimated peak metamorphic conditions for Mt. Riiser-Larsen and Tonagh Island at about 1050–1100°C, and pointed out that the area around Amundsen Bay represents a generally high-temperature regime. A similar high-temperature condition is estimated for the Howard Hills area, and it is suggested that the ultrahigh-temperature metamorphism extended over the entire area of Tonagh Island, Mt Riiser-Larsen and the Howard Hills, and perhaps beyond. The estimated P-T condition for the garnet-orthopyroxene equilibrium pair (both core composition) in type-B aluminous gneiss, using the compositional isopleths of Hensen and Harley (1990), ranges from 850 to 950°C and 8 to 9 kbar It is recognized, however, that these pairs may not represent an equilibrium state, owing to their retrograde diffusion effects while cooling from peak metamorphism (Fig. 17) The temperatures and pressure conditions calculated using the garnet-orthopyroxene geothermometer (Sen and Bhattacharya, 1984, Lee and Ganguly, 1988) and

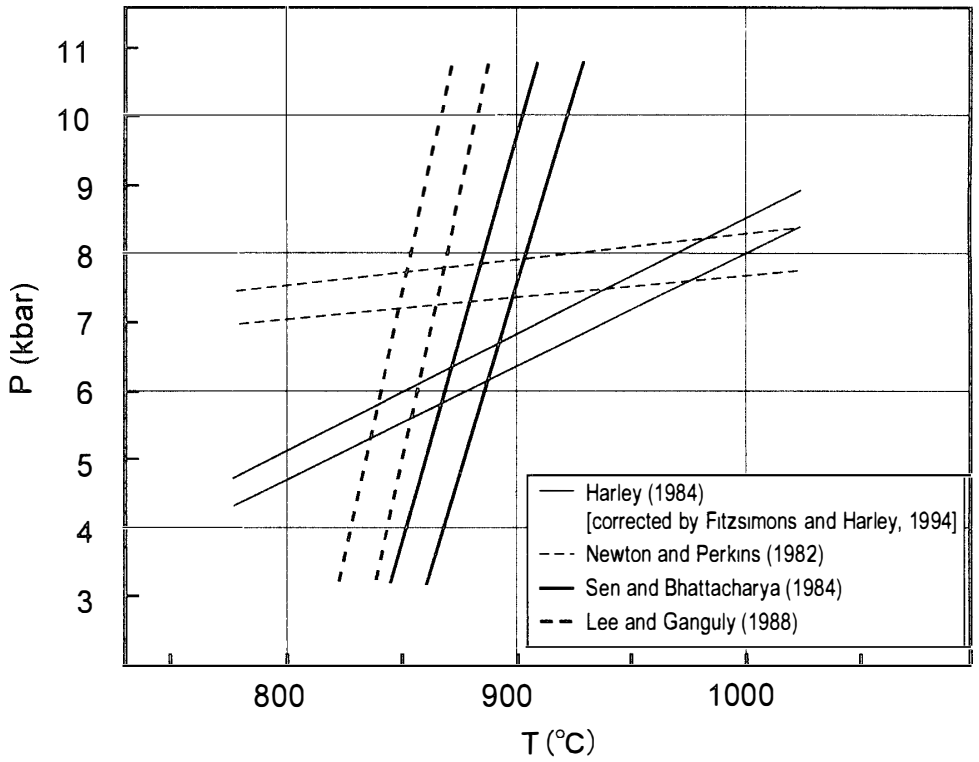

Fig 18 P-T conditions for retrograde metamorphism are estimated using garnet-orthopyroxene geothermobarometry

garnet-orthopyroxene geobarometry (Newton and Perkins, 1982, Harley, 1984, corrected by Fitzsimons and Harley, 1994) yielded from 830 to 900°C and 5 to 8 kbar (Fig 18) In general, the degree of modification of garnet composition during high temperature metamorphism is greater than that of orthopyroxene (*e.g* , Ganguly *et al* , 1998, Smith and Barron, 1991) The composition of garnets coexisting with orthopyroxene has a lower X_{Mg} value than the calculated equilibrium composition (Fig 17) Therefore, the garnet seems to have acquired this composition at a relatively low temperature, because Mg in the garnet is easy to diffuse These P-T estimates seem to show the P-T trajectory during retrograde metamorphism

4.2 Possibility of partial melting

Quartz is often included in the cores of garnets in the silica-undersaturated (quartz absent) layers of types-A and -B aluminous gneiss These quartz inclusions indicate that the media around the garnet changed from silica-oversaturated condition during garnet crystal growth to silica-undersaturated condition after garnet crystallization Therefore, the aluminous gneiss has clearly experienced mass transfer Mass transfer by partial melting is suggested by the high Y contents in garnet cores of type-A aluminous gneisses, high An values of plagioclase in the type-A aluminous gneiss and in the aluminous layer of type-B aluminous gneiss, and high Ba content in the mesoperthite in the type-A aluminous gneiss HREE such as Y and Yb concentrate in garnet when garnet coexists with melt (Rollinson, 1993) Y concentration in garnet is possibly the result of break-down of the Y-enriched phase, such as xenotime and apatite (Lanzirotti, 1995) or partial

melting (Spear and Kohn, 1996) The Y-enrichment in the garnet should take place at the same time as the composition change from silica-oversaturated to silica-undersaturated Although Ba is generally an incompatible element, the mesoperthite possibly coexisted with the melt at high temperature, because Ba becomes compatible with the crystal structure of potassium feldspar at high temperature (Rollinson, 1993). The Y_2O_3 content of garnet, the An value of plagioclase, and the BaO content of K-feldspar lamella in mesoperthite of the aluminous layer of type-B aluminous gneisses show intermediate values between that of the type-A aluminous gneiss and those of the garnet felsic gneiss and type-C aluminous gneiss. Although the Howard Hills region experienced ultrahigh-temperature metamorphism with peak temperature conditions over 1000°C, the type-A aluminous gneiss and the aluminous layers of type-B aluminous gneiss show non-equilibrium textures with regard to trace element concentration, such as zoning of Y and Yb in the garnet and variable BaO content in mesoperthite from domain to domain The timing and partial melting reaction and process involved require careful consideration Migmatite is not present in the Howard Hills The melt might have segregated completely from the host rock if partial melting took place during prograde metamorphism Then, mass transfer would have taken place in the host rock, changing the bulk composition Type-A and -B aluminous gneisses probably became enriched in Al and Mg and depleted in SiO_2 during this process It is possible that partial melt was generated from type-A and -B aluminous gneisses during prograde metamorphism, and subsequently segregated, whereas the restite might have undergone ultrahigh-temperature metamorphism

Acknowledgments

We would like to sincerely thank all members of JARE-40, all crew members of the icebreaker "Shirase", and especially Y. Ohashi, K Maki, S Harigai, T Takei and Dr H Yamauchi for their help in the helicopter operation Thanks are also due to Prof H Ishizuka and Dr T Hokada for their helpful discussion, and to Dr Y. Osanai and an anonymous reviewer for critical reading of the manuscript

References

Asami, M , Suzuki, K , Adachi, M and Grew, E S (1998) CHIME ages for granulites from the Napier Complex, East Antarctica Polar Geosci , **11**, 174-201

Bertrand, P , Ellis, D J and Green, D H (1991) The stability of sapphirine-quartz and hypersthene-sillimanite-quartz assemblages an experimental investigation in the system FeO-MgO-Al_2O_3-SiO_2 under H_2O and CO_2 conditions Contrib Mineral Petrol , **108**, 55-71

Black, L P , Williams, I S and Compston, W (1986) Four zircon ages from one rock the history of a 3930 Ma-old granulite from Mount Sones, Antarctica Contrib Mineral Petrol , **94**, 427-437

Elkins L T and Grove, T L (1990) Ternary feldspar experiments and thermodynamic models Am Mineral , **75**, 544-559

Fitzsimons, I C W and Harley, S L (1994) The influence of retrograde cation exchange on granulite P-T estimates and a convergence technique for the recovery of peak metamorphic conditions J Petrol , **35**, 543-576

Ganguly, J , Cheng, W and Chakraborty, S (1998) Cation diffusion in aluminosilicate garnets experimental determination in pyrope-almandine diffusion couples Contrib Mineral

Petrol , **131**, 171-180
Grew, E S and Manton, W I (1979) Archean rocks in Antarctica 2 5 billion-year uranium-lead ages of pegmatites in Enderby Land, Antarctica Science, **206**, 443-445
Harley, S L (1984) The solubility of alumina in orthopyroxene coexisting with garnet in FeO-MgO-Al_2O_3-SiO_2 and CaO-FeO-MgO-Al_2O_3-SiO_2 J Petrol , **25**, 665-696
Harley, S L and Hensen, B J (1990) Archaean and Proterozoic high-grade terranes of East Antarctica (40-80°E) A case study of diversity in granulite facies metamorphism High-Temperature Metamorphism and Crustal Anatexis, ed by J R Ashworth and M Brown London, Unwin Hyman, 320-370
Hensen, B J and Green, D H (1973) Experimental study of the stability of cordierite and garnet in pelitic compositions at high pressure and temperatures III Synthesis of experimental data and geological applications Contrib Mineral Petrol , **38**, 151-166
Hensen, B J and Harley, S L (1990) Graphical analysis of P-T-X relations in granulite facies metapelites High-Temperature Metamorphism and Crustal Anatexis, ed by J R Ashworth and M Brown London, Unwin Hyman, 19-56
Higgins, J B , Ribbe, P H and Herd, R K (1979) Sapphirine I Crystal chemical contricutions Contrib Mineral Petrol , **68**, 349-356
Hokada, T , Osanai, Y , Toyoshima, T , Owada, M , Tsunogae, T and Crowe, W A (1999a) Petrology and metamorphism of sapphirine bearing aluminous gneiss from Tonagh Island in the Napier Complex, East Antarctica Polar Geosci , **12**, 49-70
Hokada, T , Ishikawa, M , Ishizuka, H , Osanai, Y and Suzuki, S (1999b) Alkali feldspar compositions of the Archaean Napier Complex, East Antarctica Further evidence for 1100°C ultrahigh-temperature crustal metamorphism Abst 8th Int Symp Antarct Earth Sci , Wellington (New Zealand), 144
Ishizuka, H , Ishikawa, M , Hokada, T and Suzuki, S (1998) Geology of the Mt Riiser-Larsen area of the Napier Complex, Enderby Land East Antarctica Polar Geosci , **11**, 157-173
Kroll, H , Evangelakakis, C and Voll, G (1993) Two-feldspar geothermometry a review and revision for slowly cooled rocks Contrib Mineral Petrol , **144**, 510-518
Lanzirotti, A (1995) Yttrium zoning in metamorphic garnets Geochem Cosmoch Acta, **59**, 4105-4110
Lee, H Y and Ganguly, J (1988) Equilibrium compositions of coexisting garnet and orthopyroxene Experimental determinations in the system FeO-MgO-Al_2O_3-SiO_2, and applications J Petrol , **29**, 93-113
Newton, R C and Perkins, D (1982) Thermodynamic calibration of geobarometers based on the assemblages garnet-plagioclase-orthopyroxene (clinopyroxene)-quartz Am Mineral , **67**, 203-222
Osanai, Y , Toyoshima, T , Owada, M , Tsunogae, T , Hokada, T and Crowe, W A (1999) Geology of ultrahigh-temperature metamorphic rocks from Tonagh Island in the Napier Complex, Endarby Land, East Antarctica Polar Geosci , **12**, 1-28
Owada, M , Osanai, Y and Kagami, H (1994) Isotopic equilibration age of Sm-Nd whole rock system in the Napeir Complex (Tonagh Island), East Antarctica Proc NIPR Symp Antarct Geosci , **7**, 122-132
Owada, M , Osanai, Y , Toyoshima, T , Tsunogae, T , Hokada, T and Crow, W A (1999) Petrography and geochemistry of mafic and ultramafic rocks from Tonagh Island in the Napier Complex, East Antarctica A preliminary report Polar Geosci , **12**, 87-100
Rollinson, H (1993) Using Geochemical Data Evaluation, Presentation, Interpretation Longman, 352 p
Sen, S K and Bhattacharya, A (1984) An orthopyroxene-garnet thermometer and its application to the Madras charnockites Contrib Mineral Petrol , **88**, 64-71
Sheraton, J W , Tingey, R J , Black, L P , Offe, L A and Ellis, D J (1987) Geology of Enderby Land and Western Kemp Land, Antarctica BMR Bull , **223**, 51 p
Shiraishi, K , Ellis, D J , Fanning, C M , Hiroi, Y , Kagami, H and Motoyoshi, Y (1997) Re-

examination of the metamorphic and plotolith ages of Rayner Complex, Antarctica evidence for the Cambrian (Pan-African) regional metamorphic event The Antarctic Region Geological Evolution and Processes, ed by C A Ricci Siena, Terra Antarct Publ, 79-88

Smith, D and Barron, B R (1991) Pyroxene-garnet equilibration during cooling in the mantle Am Mineral, **76**, 1950-1963

Spear, F S and Kohn, M J (1996) Trace element zoning in garnet as a monitor of crustal melting Geology, **24**, 1099-1102

Suzuki, S, Hokada, T, Ishikawa, M and Ishizuka, H (1999) Geochemical study of granulite from Mt Riiser-Larsen, Enderby Land, East Antarctica Implication for protolith of the Archean Napier Complex Polar Geosci, **12**, 101-125

Tainosho, Y, Kagami, H, Takahashi, Y, Iizumi, S, Osanai, Y and Tsuchiya, N (1994) Preliminary result for the Sm-Nd whole-rock age of the of the metamorphic rocks from Mount Pardoe in the Napier Complex, East Antarctica Proc NIPR Symp Antarct Geosci, **7**, 115-121

Toyoshima, T, Osanai, Y, Owada, M, Tsunogae, T, Hokada, T and Crowe, W A (1999) Deformation of ultrahigh-temperature metamorphic rocks from Tonagh Island in the Napier Complex, East Antarctica Polar Geosci, **12**, 29-48

Tsunogae, T, Osanai, Y, Toyoshima, T, Owada, M, Hokada, T and Crowe, W A (1999) Metamorphic reaction and preliminary *P-T* estimates of ultrahigh-temperature mafic granulite from Tonagh Island in the Napier Complex, East Antarctica Polar Geosci., **12**, 71-86

Williams, I S, Compston, W, Black, L P, Ireland, T R and Foster, J J (1984) Unsupported radiogenic Pb in zircon a cause of anomalously high Pb-Pb, U-Pb and Th-Pb ages Contrib Mineal Petrol, **88**, 322-327

(Received April 20, 2000, Revised manuscript accepted July 21, 2000)